

# Microbial species interactions determine community diversity in fluctuating environments

Shota Shibasaki<sup>1</sup>, Mauro Mobilia<sup>2</sup>, and Sara Mitri<sup>1</sup>

<sup>1</sup>Department of Fundamental Microbiology, University of Lausanne, Switzerland

<sup>2</sup>Department of Applied Mathematics, School of Mathematics, University of Leeds, United Kingdom

E-mail addresses of all authors.

SS: shota.shibasaki@unil.ch

MM: M.Mobilia@leeds.ac.uk

SM: sara.mitri@unil.ch

Short running title: Microbial diversity under fluctuation

Key words: competitive exclusion, environmental switching, demographic noise, chemostat, beta diversity, intermediate disturbance hypothesis

Type of article: article

Numbers of words: 150 words in abstract, and 5052 words in main text.

Number of references: 53.

Numbers of figures: 4, tables: 1, text box 0.

Corresponding author: Sara Mitri: Quartier UNIL-Sorge, Batiment Biophore, Office 2414, CH-1015 Lausanne. Phone : +41 21 692 56 12. E-mail: sara.mitri@unil.ch.

Statement of authorship: SS, MM and SM designed the study, SS performed simulations, analyzed data, and wrote the first draft, and all authors contributed to revisions.

## **Abstract**

Microorganisms often live in environments that fluctuate between mild and harsh conditions. Although such fluctuations are bound to cause local extinctions and affect species diversity, it is unknown how diversity changes at different fluctuation rates and how this relates to changes in species interactions. Here, we use a mathematical model describing the dynamics of resources, toxins, and microbial species in a chemostat where resource supplies switch. Over most of the explored parameter space, species competed, but the strength of competition peaked at either low, high or intermediate switching rates depending on the species' sensitivity to toxins. Importantly, however, the strength of competition in species pairs was a good predictor for how community diversity changed over the switching rate. In sum, predicting the effect of environmental switching on competition and community diversity is difficult, as species' properties matter. This may explain contradicting results of earlier studies on the intermediate disturbance hypothesis.

# 1 Introduction

Natural environments are not static: temperature, pH, or availability of resources change over time. Many studies in microbiology, ecology and evolution have focused on responses to fluctuations in resource abundance in the regime of feast and famine periods (Hengge-Aronis, 1993; Vasi et al., 1994; Srinivasan and Kjelleberg, 1998; Xavier et al., 2005; Merritt and Kuehn, 2018; Himeoka and Mitarai, 2019). These models capture the dynamics within many natural ecosystems. For example, the gut microbiome of a host is exposed to fluctuating resources that depend on its host’s feeding rhythm, which may affect microbiota diversity (Cignarella et al., 2018; Li et al., 2017; Thaïss et al., 2014). In addition to their magnitude, environmental fluctuations can also differ in their time scales: for the gut microbiota, a host’s feeding rhythm may vary from hourly to daily, or even monthly if feeding depends on seasonal changes (Davenport et al., 2014; Smits et al., 2017). Finally, the host does not always feed its gut flora, but may also expose it to lethal toxins through the consumption of antimicrobial treatments.

How fluctuations affect species diversity has been a highly contested topic in ecology. The intermediate disturbance hypothesis argues that intermediate intensity and frequency of disturbance maximize species diversity (Connell, 1978; Grime, 1973) because species with high competitive ability dominate at a low level of disturbance while species that adapted to the disturbance dominate at high disturbance (Grime, 1977). This hypothesis is controversial (Fox, 2013) and other relationships between disturbance and species diversity have been reported both empirically and theoretically (Mackey and Currie, 2001; Miller et al., 2011).

Another body of theory that considers how environmental fluctuations can affect species diversity is modern coexistence theory (Chesson, 1994). In modern coexistence theory, spatial and temporal differences in the environment mediate species coexistence when species differ in their preferences for environmental conditions and/or in their response to fluctuations in factors like resources and toxins (Amarasekare, 2019; Chesson, 2000a,b; Letten et al., 2018b; Barabás et al., 2018; Ellner et al., 2019). Resources and toxins have opposite effects on growth rates: consumption of resources by other species decreases the growth rate of a focal species (competition/exploitation) while absorption of toxin by others can increase its growth rate (facilitation). This implies that environmental conditions, especially amounts of resources and toxins, can affect the sign and/or magnitude of species interactions (Hoek et al., 2016; Piccardi et al., 2019; Zuñiga et al., 2019). In turn, how pairs of species in a community interact (i.e., competition or facilitation) affects species diversity and community stability (Mougi and Kondoh, 2012; Coyte et al., 2015). Environmental fluctuations in nutrient and toxin concentrations are therefore expected to affect species interactions, which should then affect community diversity.

Recently, Rodríguez-Verdugo et al. (2019) used theory and experiments to show that the rate of environmental fluctuations affects the coexistence of two species when the environment switches between two carbon sources that promote either exploitation or competition between the species. However, it is unclear whether and how environmental fluctuations in amounts of – rather than types of – resources affect species coexistence and diversity because we do not know how species interactions change *a priori*. More generally, we ask: can

one predict patterns of diversity under fluctuating environments in larger communities composed of more than two species? How do these changes in diversity relate to changes in inter-species interactions? And how do environmental conditions (e.g., resource or toxin concentrations) affect these changes?

To shed light on these questions, we develop a mathematical model to investigate how the rate of environmental fluctuations affects species interactions and diversity. We start with a simple scenario with just two species in an environment that switches between scarce and abundant resource supplies. In addition to resources, our model includes the dynamics of toxins, as we expect them to affect inter-species interactions (Hoek et al., 2016; Piccardi et al., 2019; Zuñiga et al., 2019). Accordingly, the two species can both compete for resources and facilitate each other by absorbing toxic compounds. We focus on the faster grower and ask: (i) How often does this species go extinct due to the presence of a slower-growing species, and (ii) how does such extinction depend on the environmental switching rate and other properties of the environment? For most parameter values, the faster grower’s extinction probability increases because of competitive exclusion by the slower grower. To our surprise, we found that this competitive effect peaked at different switching rates depending on environmental toxicity. Second, to verify whether these findings generalize to, and predict the dynamics of larger community dynamics, we simulated communities of up to 10 species and found a similar pattern: beta diversity was highest at different switching rates in different environments. Although various relationships between disturbance and diversity have been previously reported (Mackey and Currie, 2001; Miller et al., 2011), our model associates the strength of competition between two species with the loss of beta diversity in a larger community in a fluctuating environment. In other words, to estimate how beta diversity changes over the environmental switching rate, it may be sufficient to analyze the sign and strength of interactions between two representative species under those same conditions.

## 2 Model

In this paper, we analyze how environmental switching rate  $\nu$  affects species interactions and diversity in a chemostat model. For simplicity, we assume symmetric random switching (but see Taitelbaum et al. (2020) for asymmetric, random and periodic switching). This model combines two sources of noise: birth and death events occur randomly yielding demographic noise, while the environment randomly switches from being harsh to mild and vice versa and drives the population size (Wienand et al., 2017, 2018; West and Mobilia, 2020; Taitelbaum et al., 2020). When the environment becomes harsh (e.g., abundant toxins or scarce resources), the population shrinks and demographic noise can lead to extinction. As in previous work, a distinctive feature of this model is therefore the coupling of demographic and environmental noise: environmental switching changes the population size, which in turn modulates demographic fluctuations, which results in feedback loops. Here, we implement environmental switching by modeling time-varying resource and/or toxin supplies, as we are interested in how these environmental conditions mediate species interactions and diversity.

Our model includes the dynamics of the amount  $r_i$  of resource  $i$  ( $i = 1, \dots, N/2$ , where  $N$  is an even number) that allows all species to grow, the amount  $t_j$  of toxic compound  $j$  ( $j = 1, \dots, N/2$ ) that kills all species, and the

abundance  $s_k$  of species  $k$  ( $k = 1, \dots, N$ ). When  $N = 2$  species, we recapitulate the environmentally mediated species interactions shown in the model of [Piccardi et al. \(2019\)](#), where species affect each other positively in toxic environments, with increasing competition in more benign environments. The dynamics are modelled in terms of a multivariate continuous-time birth-and-death process (see [Novozhilov et al. \(2006\)](#); [Allen \(2010\)](#) for example) defined by the following “birth” and “death” reactions:



occurring with transition rates:

$$\tau_{r_i}^+ = \alpha R_i(\xi), \quad (2a)$$

$$\tau_{r_i}^- = \sum_{k=1}^N \frac{\mu_{ik}}{Y_{ik}^r} \frac{r_i}{r_i + K_{ik}^r} s_k + \alpha r_i, \quad (2b)$$

$$\tau_{t_j}^+ = \alpha T_j(\xi), \quad (2c)$$

$$\tau_{t_j}^- = \sum_{k=1}^N \frac{\delta_{jk}}{Y_{jk}^t} \frac{t_j}{t_j + K_{jk}^t} s_k + \alpha t_j, \quad (2d)$$

$$\tau_{s_k}^+ = \sum_{i=1}^{N/2} \mu_{ik} \frac{r_i}{r_i + K_{ik}^r} s_k, \quad (2e)$$

$$\tau_{s_k}^- = \sum_{j=1}^{N/2} \delta_{jk} \frac{t_j}{t_j + K_{jk}^t} s_k + \alpha s_j, \quad (2f)$$

where  $\alpha$  is the dilution rate of the chemostat,  $\xi = \pm 1$  (see below) represents changing environmental conditions in terms of in-flowing resource and/or toxin concentration,  $R_i(\xi)$  ( $T_j(\xi)$ ) is resource  $i$ 's (toxin  $j$ 's) supply under the environmental condition  $\xi$ ,  $Y_{ik}^r$  ( $Y_{jk}^t$ ) is species  $k$ 's biomass yield for resource  $i$  (toxin  $j$ ),  $\mu_{ik}$  is the maximum growth rate of species  $k$  by resource  $i$ ,  $\delta_{jk}$  is the maximum death rate of species  $k$  by toxin  $j$  (species  $k$ 's sensitivity to toxin  $j$ ), and  $K_{ik}^r$  ( $K_{jk}^t$ ) is the amount of resource  $i$  (toxin  $j$ ) that gives the half-maximum growth (death) rate of species  $k$ . In this model, we assume that growth and death rates depend on the amounts of resource and toxin in Monod function forms, respectively, and that the effects are additive.

Environmental switching changes resource and/or toxin supplies at rate  $\nu$  according to

$$\xi \xrightarrow{\nu} -\xi, \quad (3)$$

where  $\xi \in \{-1, +1\}$  is a coloured dichotomous (telegraph) noise assumed to be symmetric and stationary (Bena, 2006; Horsthemke and Lefever, 2006). Here, the mean of  $\xi(t)$  is therefore always zero and its finite correlation time is  $1/\nu$ . One can imagine three environmental switching scenarios, where either or both resource and toxin supplies change (Table 1). In the main text, we analyze only scenario 1 where only resource supplies switch, but see Appendix 4 for the remaining scenarios. When environmental switching affects the resource supply  $R_i$ , it switches between abundant and scarce:

$$R_i(\xi) = \begin{cases} R_i^+ & \xi = 1 \text{ (abundant)} \\ R_i^- & \xi = -1 \text{ (scarce)} \end{cases} \quad \text{s.t. } R_i^+ > R_i^- > 0, \forall i. \quad (4)$$

It is clear that (2a)-(4) define a multivariate birth-and-death process *coupled* with environmental switching. As environmental switching does not affect toxin supply in this scenario, the mean amount of toxins is supplied  $\langle T_j \rangle$ , where  $\langle \cdot \rangle$  represents the mean of abundant and scarce supplies of a focal resource or toxin (e.g.,  $\langle T_j \rangle \equiv (T_j^+ + T_j^-)/2$  such that  $T_j^+ > T_j^- > 0, \forall j$ ).

Note that when demographic noise is ignored, the sole source of randomness stems from the dichotomous Markov noise, which clearly results in the waiting time between two environmental switches to be exponentially distributed with a mean  $1/\nu$  (Bena, 2006). In the joint presence of demographic noise and environmental switching, see, e.g., (Hufton et al., 2016; West et al., 2018), the waiting time approximately follows the exponential distribution with mean  $1/\nu$ , with the larger the switching rate the shorter the sojourn in either of the environmental states.

The master equation for this model is defined by combining the dynamics of amount of resources and toxins, abundances of species, and environmental switching (Eqs (1a) - (3)):

$$\begin{aligned} \dot{P}(\vec{r}, \vec{t}, \vec{s}, \xi) = & \sum_{i=1}^{N/2} (\mathbb{E}_{r_i}^- - 1) \{ \tau_{r_i}^+ P(\vec{r}, \vec{t}, \vec{s}, \xi) \} \\ & + \sum_{i=1}^{N/2} (\mathbb{E}_{r_i}^+ - 1) \{ \tau_{r_i}^- P(\vec{r}, \vec{t}, \vec{s}, \xi) \} \\ & + \sum_{j=1}^{N/2} (\mathbb{E}_{t_j}^- - 1) \{ \tau_{t_j}^+ P(\vec{r}, \vec{t}, \vec{s}, \xi) \} \\ & + \sum_{j=1}^{N/2} (\mathbb{E}_{t_j}^+ - 1) \{ \tau_{t_j}^- P(\vec{r}, \vec{t}, \vec{s}, \xi) \} \\ & + \sum_{k=1}^N (\mathbb{E}_{s_k}^- - 1) \{ \tau_{s_k}^+ P(\vec{r}, \vec{t}, \vec{s}, \xi) \} \\ & + \sum_{k=1}^N (\mathbb{E}_{s_k}^+ - 1) \{ \tau_{s_k}^- P(\vec{r}, \vec{t}, \vec{s}, \xi) \} \\ & + \nu \{ P(\vec{r}, \vec{t}, \vec{s}, -\xi) - P(\vec{r}, \vec{t}, \vec{s}, \xi) \} \end{aligned} \quad (5)$$

where  $P(\vec{r}, \vec{t}, \vec{s}, \xi)$  represents the probability density of  $\vec{r} = (r_i)$ ,  $\vec{t} = (t_j)$ ,  $\vec{s} = (s_k)$ , and  $\xi$ , the dot denotes the

time derivative, and  $\mathbb{E}_{r_i}^\pm$  is a shift operator such that

$$\mathbb{E}_{r_i}^\pm P(\vec{r}, \vec{t}, \vec{s}, \xi) = P(r_1, \dots, r_i \pm 1, \dots, r_{N/2}, \vec{t}, \vec{s}, \xi), \quad (6)$$

and  $\mathbb{E}_{t_j}^\pm$  and  $\mathbb{E}_{s_k}^\pm$  are the equivalent shift operators for  $t_j$  and  $s_k$ , respectively. The last line on the right-hand-side of (5) accounts for the random switching reaction (3). The model given by Eq. (5) was implemented using the Gillespie algorithm (Gillespie, 1977) until, after a sufficiently large time  $T_{end}$ , the population size distribution converges to a quasi-stationary distribution (i.e., where distributions of species abundances appear to be stationary for a long time; the real equilibrium state corresponding to the extinction of all species being practically unobservable). In two species scenarios, either or both two species go extinct before time  $T_{end}$  in most cases (see Fig. 4 column C.). For details on parameter values and the simulations, see Appendix 2. A schematic illustration of this model with  $N = 2$  is summarized in Fig. 1.

## 2.1 Evaluating species interactions

We begin by analyzing interactions between two species ( $N = 2$ ) where the sign and magnitude of species interactions can change. We used parameter values such that species 1 always outcompetes species 2 in a deterministic and fixed environment setting (i.e., species 1 grows faster than species 2, see Appendix 1 for analysis and Table A.1 for exact parameter values) to clarify the effects of demographic noise. Under demographic noise coupled with environmental switching, either of the two species or both species tend to go extinct. As a proxy for interactions, we focus on the net effect of species 2 on species 1, which is defined by the extinction probability of species 1 in mono-culture minus that in co-culture with species 2:

$$\Delta P(s_1(T_{end}) = 0) \equiv P(s_1(T_{end}) = 0; s_2(0) = 0) - P(s_1(T_{end}) = 0; s_2(0) > 0). \quad (7)$$

If  $\Delta P(s_1(T_{end}) = 0)$  is  $< -0.01$ , we consider that species 2 increases the extinction probability of species 1 (negative effect), whereas  $\Delta P(s_1(T_{end}) = 0) > 0.01$  implies that species 2 has a positive effect on species 1. We ignore small values of  $|\Delta P(s_1(T_{end}) = 0)|$ , as they are biologically meaningless and may be due to the finite number of simulations.

In the analysis of species diversity (see below) with  $N = 2$ , we also analyzed the species interactions in 100 pairs of species that differ in  $\mu_{ik}$ ,  $K_{ik}^r$ ,  $\delta_{jk}$ , and  $K_{jk}^t$  in the presence of demographic noise and environmental switching. Since pairs of species may coexist depending on their parameter values in the diversity analysis, species 1 (or 2) is the one that has larger (or smaller) population size than the other in the absence of any noise. If both species go extinct in the absence of noise, species 1 is chosen randomly.

## 2.2 Evaluating species diversity

To explore how species diversity changes over switching rates, we ran simulations at different community sizes ranging from  $N = 2$  to  $N = 10$  and different mean toxin sensitivities, from  $\bar{\delta} = 0.1$  to  $\bar{\delta} = 1$ . For each

condition (one  $N$  and one  $\bar{\delta}$ ), we sampled 100 sets of parameters  $\mu_{ik}$ ,  $K_{ik}^r$ ,  $\delta_{jk}$ , and  $K_{jk}^t$ , which represented 100 meta-communities composed of  $N$  species whose differences were reflected in the parameter values. Each meta-community had 100 independent communities (no inter-community migration and independent environmental switching) with equal initial species abundances. In short, we replicated 100 simulations for each of 100 sets of parameter values, and we had in total 10,000 simulations for each combination of community size, mean toxin sensitivity, and switching rate.

Because demographic noise and environmental switching affect species composition, we investigated the heterogeneity of communities at the end of each simulation run. We measured beta diversity (Jost, 2007; Chao et al., 2012) of each meta-community and species richness (number of surviving species) for each community at a quasi-stationary state ( $T_{end}$ ):

$${}^1D_{\beta}(T_{end}) \equiv \frac{{}^1D_{\gamma}(T_{end})}{{}^1D_{\alpha}(T_{end})}, \quad (8)$$

with alpha and gamma diversities defined as below:

$${}^1D_{\alpha}(T_{end}) \equiv \exp\left(-\sum_{l=1}^{100} \sum_{k=1}^N w_l p_{lk}(T_{end}) \ln p_{lk}(T_{end})\right), \quad (9)$$

$${}^1D_{\gamma}(T_{end}) \equiv \exp\left(-\sum_{k=1}^N \bar{p}_k \ln \bar{p}_k(T_{end})\right). \quad (10)$$

$w_l$  is a weight for community  $l$  calculated by size of community  $l$  (sum of species abundances in community  $l$  relative to the sum of community sizes over  $l$ ),  $p_{lk}$  is the relative abundance of species  $k$  in community  $l$  (i.e., in community  $l$ ,  $p_{lk}(T_{end}) = s_k(T_{end}) / \sum_k s_k(T_{end})$ ), and  $\bar{p}_k = \sum_l w_l p_{lk}$  is the mean relative abundance of species  $k$  among communities  $l = 1, \dots, 100$ . If all species go extinct in community  $l$ , it does not affect alpha, beta and gamma diversities as  $w_l = 0$ . If all species go extinct in all communities, beta diversity becomes  ${}^1D_{\beta}(T_{end}) = 1$ . For more detail, see [Appendix 2](#).

## 2.3 Statistical analysis

Statistical analysis was performed with Python 3.7.6 and Scipy 1.4.1. For statistical tests of Spearman's rank-order correlation, `scipy.stats.spearmanr` was used.

# 3 Results

## 3.1 Toxin sensitivity changes how switching rate affects species interactions

Our aim is to investigate how species interactions and diversity change over the environmental switching rate. Rather than measuring interactions through the effect of each species on the other's biomass, we focus on a fast-growing species (that we call species 1) and analyze how its extinction probability is affected by the presence of a second slower-growing species (species 2). Our reasoning here is that in the absence of noise, species 1



should always out-compete species 2, so measuring any deviation from this outcome allows us to quantify the effect of coupled demographic noise and environmental fluctuations. We explored how this proxy for species interactions was affected by different environmental switching rates as well as different toxin sensitivities, which we varied simultaneously for both species, such that the species were always equally sensitive to the toxin.

When both species were highly sensitive to the toxin (large  $\delta$ ), species 2 has a positive effect on species 1. This occurs because species 2 also degrades the toxin, which outweighs the competition for nutrients (Piccardi et al., 2019). However, for most parameter values in Fig. 2A, species 2 has a negative effect on species 1 by increasing its extinction probability. We therefore focus on competitive interactions (i.e.,  $\Delta P(s_1(T_{end}) = 0) < 0$ ) for the remainder of the main part of the study and consider positive interactions in Appendix 5.

As we varied the switching rate, we observed that the strength of the competitive effect was highly dependent on the toxin sensitivity  $\delta$  of the two species: monotonically increasing, monotonically decreasing, or non-monotonically changing with a minimum or maximum value at an intermediate switching rate (Fig. 2B). How our system behaves under the two extreme switching rates becomes clear if one considers what happens in the absence of environmental switching (Fig. A.3). At very low rate  $\nu \rightarrow 0$ , there are almost no switches: the environment remains either poor or rich in nutrient (probability 1/2) and microbes are as likely to experience either scarce or abundant resources from  $t = 0$  until  $t = T_{end}$ . The outcome at this switching rate therefore corresponds to the mean outcome of those two environments. On the other hand, a very fast environmental switching rate ( $\nu \rightarrow \infty$ ) corresponds to a scenario where the resource supply is at mean concentration (environmental noise self averages, see, e.g., Wienand et al. (2017, 2018); West and Mobilia (2020); Taitelbaum et al. (2020)). How the strength of competition varies at an intermediate switching rate is, however, less intuitive. We explore this next.

### 3.2 Competitive exclusion explains negative species interactions

To better understand the unexpected changes in the effect of species 2 on species 1 (Fig. 2B), we analyse our proxy for species interactions in more detail.  $\Delta P(s_1(T_{end}) = 0)$  represents the difference between the probability of species 1 going extinct in mono-culture ( $P(s_1(T_{end}) = 0; s_2(0) = 0)$ ) versus in co-culture with species 2 ( $P(s_1(T_{end}) = 0; s_2(0) > 0)$ ) (Eq. 7). By decomposing the co-culture component into two probabilities depending on whether species 2 persists or not and rearranging the equation, we obtain:

$$\Delta P(s_1(T_{end}) = 0) = - \underbrace{P(s_1(T_{end}) = 0, s_2(T_{end}) > 0; s_2(0) > 0)}_{\text{competitive exclusion}} + \left\{ \underbrace{P(s_1(T_{end}) = 0; s_2(0) = 0)}_{\text{sp 1 goes extinct in mono-culture}} - \underbrace{P(s_1(T_{end}) = 0, s_2(T_{end}) = 0; s_2(0) > 0)}_{\text{both species go extinct}} \right\}. \quad (11)$$

The first line of Eq (11) represents the probability that species 2 excludes species 1 and survives (competitive exclusion), while the second line is species 1's extinction probability in mono-culture minus the probability of

both species going extinct.

Fig. A.2 shows that the overall interaction strength is not affected much by the second line of Eq (11), and that the competitive exclusion probability explains the variation in species interaction strength in most cases (compare Fig. 2A and C). Intuitively, this is because under the environmental conditions where both species are likely to go extinct (i.e., small resource supplies and high toxin sensitivity), species 1 is also likely to go extinct in mono-culture, resulting in a small magnitude of the second line of Eq (11). For this reason, the competitive exclusion probability changes similarly to the effect of species 2 on species 1 over environmental switching rates and toxin sensitivities (Fig. 2C). In other words, we can assume that the second line of Eq (11) is negligible and focus instead on the competitive exclusion probability.

### 3.3 Competitive exclusion explains non-monotonic changes in species interactions

Following the logic outlined above, we now use the competitive exclusion probability to investigate why the strength of negative interactions changes over the switching rate in various ways, depending on toxin sensitivity.

In the absence of environmental switching, the competitive exclusion probability is uni-modal over toxin sensitivity  $\delta$ , regardless of the resource supply (Fig. 3A). As a reminder, competitive exclusion implies the extinction of species 1 and the survival of species 2. Since toxin sensitivity is identical for both species, when toxin sensitivity is too high, both species are likely to go extinct (Fig. A.4), which does not count as competitive exclusion. Instead, competitive exclusion is most likely at lower toxin sensitivities whose value depends on the amount of resource supply: when more resources are supplied, the peak moves to a higher toxin sensitivity because species are more likely to survive (Fig. 3A). Hereafter, we refer to the toxin sensitivity that maximizes the competitive exclusion probability in the absence of environmental switching as the “critical toxin sensitivity”.

This analysis clarifies what happens at the two extreme switching rates. At a very slow switching rate ( $\nu \rightarrow 0$ ), the environment remains for a long time with either scarce or abundant resources. Accordingly, competitive exclusion has two peaks over the toxin sensitivity (at  $\delta = 0.1$  and  $0.8$  in Figs. 2C and D) corresponding to the critical toxin sensitivities under the scarce and abundant resource supplies in Fig. 3A, respectively. On the other hand, at very fast switching rates ( $\nu \rightarrow \infty$ ), where resources remain at mean abundance, competitive exclusion has one peak (at  $\delta = 0.4$  in Figs. 2C and D) corresponding to the critical toxin sensitivity under the mean resource supply in Fig. 3A. In sum, the form of the competitive exclusion probability in Fig. 2C changes from bi-modal to uni-modal by increasing the switching rate.

The non-monotonic change of competitive exclusion probability over the switching rate can happen at toxin sensitivities between the critical toxin sensitivities under scarce (or abundant) and mean resource supplies (Fig. 2C). This phenomenon can be explained by considering that the landscape of competitive exclusion depicted in Fig. 2C contains two “mountain ranges”. The first “mountain range” includes two peaks corresponding to the critical toxin sensitivities under the scarce and mean resource supplies ( $\delta = 0.1, 0.4$ , respectively). By increasing environmental switching from a very slow rate, the peak at  $\delta = 0.1$  converges to the peak at  $\delta = 0.4$  (Fig. 2D). The second “mountain range” consists of the peak corresponding to the critical toxin sensitivity under the

abundant resource supply ( $\delta = 0.8$ ). This peak vanishes by increasing the switching rate (Fig. 2D).

At toxin sensitivities between critical values under scarce and mean resource supplies ( $\delta = 0.2, 0.3$ ), the competitive exclusion probability changes in a humped shape over the switching rate (species interactions change in a U shape, see Fig. 2B). This is because an intermediate switching rate has a peak of competitive exclusion probability belonging to the first mountain range. When the toxin sensitivity is  $\delta = 0.6$ , the environmental switching rate also non-monotonically affects the competitive exclusion probability, but for a different reason. Toxin sensitivities between the critical values under mean and abundant resource supplies can have a “valley” over the switching rate: at such toxin sensitivities, competitive exclusion probability changes in a U shape over the switching rate (species interactions change in a humped shape, see Fig. 2B). At toxin sensitivities larger than the critical value under the abundant resource supply, competitive exclusion probability is very small and does not change non-monotonically over the switching rate because both species frequently go extinct (Fig A.4).

### 3.4 Non-monotonic changes in species interactions happen under different scenarios of environmental differences

We have shown that using a given set of parameters, the rugged landscape shown in Fig. 2C causes competition to either increase, decrease or vary non-monotonically across switching rates, depending on toxin sensitivity. We next explore the generality of this finding and ask whether it will hold under different scenarios. In the appendix, we explore scenarios where (i) switching occurs in toxin rather than resource supplies, where (ii) both resource and toxin supplies switch (Table 1, see Appendix 4), or where (iii) we change the amounts of scarce and abundant resource supplies (Appendix 5).

In all these scenarios, the landscapes of competitive exclusion probability also contain two “mountain ranges” (Figs. A.5, A.7), leading, as before, to a variety of patterns as switching rates and toxin sensitivities change. In each scenario, the distances between the three critical toxin sensitivities (mild, mean and harsh, e.g. black arrow in Fig. 3A) change (see Table A.2). Do these distances predict the shape of the landscape and the probability of observing non-monotonic behavior? In Table A.2 and Fig. 3B we show that the distance between critical sensitivities under harsh and mean environments (i.e., very fast environmental switching) correlates positively with the likelihood of observing non-monotonic effects of the switching rate on competition (Fig. 3B, black circles; Spearman’s  $\rho = 0.77$ , P-value: 0.043), but no significant correlation was found with the distance between the critical toxin sensitivities under the mean and mild, or the harsh and mild environments (Fig. 3B, grey diamonds and cross marks; Spearman’s  $\rho = -0.22$ , P-value: 0.64, and  $\rho = 0.42$ , P-value: 0.35, respectively). These differences can be explained by changes in the shape of the landscape (see subsection 3.3). In sum, we find non-monotonic behavior under many different scenarios, with no easily observable pattern for when they occur. Overall, this makes it challenging to predict how the strength of interspecific interactions will change over environmental switching rates.

### 3.5 Beta diversity changes similarly to competitive exclusion

In the previous sections, we have focused on interactions between two species and the conditions under which they may drive each other extinct. Ultimately, however, our interest is to predict how species diversity is affected by the environment in communities comprised of tens, hundreds or even thousands of species. In this section, we ask whether the same rules that we have uncovered between two species apply for larger communities of up to 10 species. Will the diversity of a community similarly depend on environmental switching rates and toxin sensitivities?

We address this question by extending our model to simulate communities of between 2 and 10 species. Simulating larger communities with this model would be too computationally expensive. As our model includes stochastic environmental switching and demographic noise, we ran 10'000 simulations for each community size and for each of 5 different mean toxin sensitivities (here species in a community could differ in their toxin sensitivity) ranging from  $\bar{\delta} = 0.1$  to  $\bar{\delta} = 1$  (see Methods). At the end of each simulation run, we measured the beta diversity and species richness (number of surviving species). These 10'000 ( $100 \times 100$ ) simulations were composed of 100 replicate runs for one of 100 randomly sampled sets of parameter values (see Methods).

In two-species communities, beta diversity changes over the environmental switching rate similarly to the competitive exclusion probability for four out of five mean toxin sensitivities (columns A and B in Fig. 4): both monotonically decrease (mean toxin sensitivity  $\bar{\delta} = 0.1$  or  $1.0$ ), or non-monotonically change with maximum ( $\bar{\delta} = 0.2$ ) or minimum ( $\bar{\delta} = 0.6$ ) values at intermediate switching rates. At one mean toxin sensitivity  $\bar{\delta} = 0.4$ , the patterns of competitive exclusion and beta diversity over the switching rate do not match. Our measure of final species richness (column C in Fig. 4) shows that at low switching rates and  $\bar{\delta} = 0.4$ , both species can sometimes co-exist, which keeps beta-diversity high. Although two species can also coexist when  $\bar{\delta} = 0.1$  or  $0.2$ , the probability of coexistence changes over the switching rate similarly to the competitive exclusion probability, leading to similar patterns in both measures.

We next increase the number of species in community to 10 (Figs. A.10 and A.11) to see whether the same patterns of beta diversity are observed. The similarity remains in 10-species communities (columns D and E in Fig. 4). Although variation in species richness increases beta diversity, the inverse is not true: beta diversity can be large when species richness is likely to be one (see  $\bar{\delta} = 0.4$  and  $0.6$  at switching rate larger than  $10^1$  in D and E columns in Fig. 4). In such cases, different species fixate in each simulation by competitive exclusion. In sum, estimating the competitive exclusion probability in two species in a given environment is a good predictor for the beta diversity of larger communities under those same environmental conditions.

## 4 Discussion

Understanding how species diversity in microbial communities arises and is maintained is a central question in microbial ecology and evolution. Diversity is affected by biotic interactions between species, but also by abiotic properties of the environment, such as its harshness (availability of nutrients and/or toxicity), and how conditions fluctuate over time. Here we have used a mathematical model to explore the relationship between

these three factors and how they affect the diversity of small communities.

Our study is centred on two main findings. First, we show that the rate at which resource abundance fluctuates in the environment changes the strength of negative interactions (competition) – quantified as the ability of a slower-growing species to drive a fast-growing one extinct. However, these changes depend strongly on how toxic the environment is for both species. As the switching rate increases, competition can monotonically increase, monotonically decrease, or change non-monotonically (Fig. 2B), depending on toxin sensitivity. These negative interactions mostly manifest themselves as competitive exclusion, rather than the extinction of both species (Figs. 2C and A.2). By calculating the critical toxin sensitivities that maximize competitive exclusion in the absence of environmental switching, one can predict how the switching rate will affect the strength of competition at a given toxin sensitivity. Our second main finding is that studying changes in the probability of two species competitively excluding one another is a good indicator for how the beta diversity of a community composed of up to 10 species will change with environmental switching (Fig. 4).

This brings us to a hypothesis that has been debated at length in ecology: the intermediate disturbance hypothesis (Connell, 1978; Grime, 1973), which states that intermediate intensity and frequency of disturbance maximize species diversity. Fox (2013) argues that the intermediate disturbance hypothesis should be abandoned because many examples disagree with it (Mackey and Currie, 2001; Miller et al., 2011). In our model, fluctuations in resource and toxin concentrations can be regarded as disturbances. In agreement with Mackey and Currie (2001) and Miller et al. (2011) then, an intermediate intensity (i.e., toxin sensitivity) or disturbance frequency (environmental switching rate) does not always maximize beta diversity: our analysis shows that intermediate frequencies of disturbance maximize beta diversity only when mean toxin sensitivity is within a certain range. Mean toxin sensitivities at the two thresholds of this range show that beta diversity monotonically decreases or increases over the switching rate. These thresholds depend on scenarios of environmental switching and amounts of resource supplies because these parameters change probability of competitive exclusion (see Appendix 4 and Appendix 5). High diversity at intermediate disturbances is then a consequence of a change in environmental conditions and not expected to apply generally.

The relationship between environmental fluctuations and species diversity is also an important question in modern coexistence theory, which predicts that fluctuations will affect species coexistence by changing species growth rates when rare (Chesson, 2000a,b; Barabás et al., 2018; Ellner et al., 2019; Letten et al., 2018a). Compared to the approach taken in this study – where we ask how many and which species persist at the end of a long but fixed time frame (i.e., for a quasi-stationary distribution, Fig. 4) – modern coexistence theory allows one to analyze whether or for how long a set of species will all coexist (Schreiber et al., 2020). An interesting future direction would be to apply modern coexistence theory to investigate how environmental fluctuation rates and toxin sensitivities affect the duration of all-species coexistence. This approach would help to propose biological mechanisms behind species coexistence in our setup.

Of course, our model makes some simplifying assumptions and has some limitations. First, we used arbitrary time units, which in practice can be considered to be hours, corresponding to typical bacterial growth rates in relevant experiments (Novick and Szilard, 1950; Lin et al., 2002; Zhao and Lin, 2003). This implies that species

interactions and beta diversity will vary when environmental switching ranges from hourly ( $\nu = 10^0$ ) to about once every four days ( $\nu = 10^{-2}$ ) on average, which is shorter than in some experimental studies (Benneir and Lenski, 1999; Rodríguez-Verdugo et al., 2019; Chen and Zhang, 2020) but not impractical. That said, under this assumption, changing an hourly to a monthly scale, for example, would have different effects on ecological dynamics. Second, the switching rate is assumed to be symmetric between abundant and scarce resources (and/or toxin supplies, see Appendix 4). One may include more than two environmental conditions or assume asymmetric environmental switching, as in work by Taitelbaum et al. (2020), who show that asymmetric switching can non-trivially change the effects of environmental switching. Third, our model focuses on competitive exclusion but other types of interactions can also affect diversity (Rodríguez-Verdugo et al., 2019). Positive interactions between pairs of species (e.g., cross-feeding), for example, might increase alpha and gamma diversities, because such interactions enable species to coexist (Sun et al., 2019). This could result in an increase in beta diversity because the extinction of one species by demographic noise, for example, increases its partner species' extinction probability. Finally, our community analysis considers up to ten microbial species, which is orders of magnitude below the size of natural microbial communities, according to genomic sampling (Gans, 2005; Roesch et al., 2007). However, it may also be reasonable to assume that species live in structured environments where they cannot possibly interact with more than a handful of other genotypes (Tecon et al., 2019). This suggests that a 10-species community may already be biologically meaningful.

In conclusion, the time scale of environmental switching affects the strength of species interactions, which results in changing beta diversity via competitive exclusion. In addition, how species interactions and beta diversity change with respect to the environmental switching rate varies and depends on how the species are sensitive to the environmental toxicity. This may be one mechanism which explains why the intermediate disturbance hypothesis does not always hold. The variety with which species interactions and beta diversity change over the switching rate means that it will be very difficult to predict how a given ecosystem, such as the gut microbiome, will behave under environmental fluctuations. Nevertheless, the similarity between how competitive exclusion plays out between two species and beta diversity at the community level means that analysing how the former changes over switching rates (as in Rodríguez-Verdugo et al. (2019), for example) may be sufficient to predict the latter. More generally, our study, along with others (Mackey and Currie, 2001; Miller et al., 2011) show that predicting how the environment shapes diversity in ecology remains a challenging problem. Nevertheless, models like the one presented here can help to disentangle the environmental factors contributing to species diversity.

## Acknowledgement

S.S. is funded by University of Lausanne and Nakajima foundation. S.M. is funded by European Research Council Starting Grant 715097 and the University of Lausanne. The authors declare no conflict of interest.

## Data accessibility

The programming codes and csv files for this manuscript are available in [Github](#).

## References

- Allen, L. J. S. *An Introduction to Stochastic Processes with Applications to Biology*. Chapman and Hall/CRC, New York, 2nd edition, 2010. ISBN 9780429184604. doi: 10.1201/b12537. URL <https://www.taylorfrancis.com/books/9781439894682>.
- Amarasekare, P. The evolution of coexistence theory. *Theoretical Population Biology*, 133:49–51, 2019. ISSN 10960325. doi: 10.1016/j.tpb.2019.09.005. URL <https://doi.org/10.1016/j.tpb.2019.09.005>.
- Barabás, G., D’Andrea, R., and Stump, S. M. Chesson’s coexistence theory. *Ecological Monographs*, 0(0):1–27, 2018. ISSN 00129615. doi: 10.1002/ecm.1302. URL <http://doi.wiley.com/10.1002/ecm.1302>.
- Bena, I. Dichotomous Markov noise: Exact results for out-of-equilibrium systems. A review. *International Journal of Modern Physics B*, 20(20):2825–2888, 6 2006. ISSN 02179792. doi: 10.1142/S0217979206034881. URL <http://arxiv.org/abs/cond-mat/0606116>.
- Benneir, A. F. and Lenski, R. E. Experimental evolution and its role in evolutionary physiology. *American Zoologist*, 39(2):346–362, 1999. ISSN 00031569. doi: 10.1093/icb/39.2.346.
- Chao, A., Chiu, C. H., Hsieh, T. C., and Inouye, B. D. Proposing a resolution to debates on diversity partitioning. *Ecology*, 93(9):2037–2051, 9 2012. ISSN 00129658. doi: 10.1890/11-1817.1. URL <http://doi.wiley.com/10.1890/11-1817.1>.
- Chen, P. and Zhang, J. Antagonistic pleiotropy conceals molecular adaptations in changing environments. *Nature Ecology & Evolution*, 2 2020. ISSN 2397-334X. doi: 10.1038/s41559-020-1107-8. URL <http://www.nature.com/articles/s41559-020-1107-8>.
- Chesson, P. Multispecies Competition in Variable Environments. *Theoretical Population Biology*, 45:227–276, 1994.
- Chesson, P. Mechanisms of Maintenance of Species Diversity. *Annual Review of Ecology and Systematics*, 31(1):343–366, 11 2000a. ISSN 0066-4162. doi: 10.1146/annurev.ecolsys.31.1.343. URL <http://www.annualreviews.org/doi/10.1146/annurev.ecolsys.31.1.343>.
- Chesson, P. General theory of competitive coexistence in spatially-varying environments. *Theoretical Population Biology*, 58(3):211–237, 2000b. ISSN 00405809. doi: 10.1006/tpbi.2000.1486.
- Cignarella, F., Cantoni, C., Ghezzi, L., Salter, A., Dorsett, Y., Chen, L., Phillips, D., Weinstock, G. M., Fontana, L., Cross, A. H., Zhou, Y., and Piccio, L. Intermittent Fasting Confers Protection in CNS Autoimmunity by Altering the Gut Microbiota. *Cell Metabolism*, 27(6):1222–1235, 2018. ISSN 19327420. doi: 10.1016/j.cmet.2018.05.006. URL <https://doi.org/10.1016/j.cmet.2018.05.006>.
- Connell, J. H. Diversity in Tropical Rain Forests and Coral Reefs. *Science*, 199(4335):1302–1309, 1978.



- Coyte, K. Z., Schluter, J., and Foster, K. R. The ecology of the microbiome: Networks, competition, and stability. *Science*, 350(6261):663–666, 2015. ISSN 0036-8075. doi: 10.1126/science.aad2602. URL <http://www.sciencemag.org/cgi/doi/10.1126/science.aad2602>.
- Davenport, E. R., Mizrahi-Man, O., Michelini, K., Barreiro, L. B., Ober, C., and Gilad, Y. Seasonal variation in human gut microbiome composition. *PLoS ONE*, 9(3), 2014. ISSN 19326203. doi: 10.1371/journal.pone.0090731.
- Ellner, S. P., Snyder, R. E., Adler, P. B., and Hooker, G. An expanded modern coexistence theory for empirical applications. *Ecology Letters*, 22(1):3–18, 1 2019. ISSN 1461-023X. doi: 10.1111/ele.13159. URL <https://onlinelibrary.wiley.com/doi/abs/10.1111/ele.13159>.
- Fox, J. W. The intermediate disturbance hypothesis should be abandoned. *Trends in Ecology & Evolution*, 28(2):86–92, 2 2013. ISSN 01695347. doi: 10.1016/j.tree.2012.08.014. URL <https://linkinghub.elsevier.com/retrieve/pii/S0169534712002091>.
- Gans, J. Computational Improvements Reveal Great Bacterial Diversity and High Metal Toxicity in Soil. *Science*, 309(5739):1387–1390, 8 2005. ISSN 0036-8075. doi: 10.1126/science.1112665. URL <https://www.sciencemag.org/lookup/doi/10.1126/science.1112665>.
- Gillespie, D. T. Exact stochastic simulation of coupled chemical reactions. *Journal of Physical Chemistry*, 81(25):2340–2361, 1977. ISSN 00223654. doi: 10.1021/j100540a008.
- Grime, J. P. Competitive Exclusion in Herbaceous Vegetation. *Nature*, 242(5396):344–347, 3 1973. ISSN 0028-0836. doi: 10.1038/242344a0. URL <http://www.nature.com/doi/10.1038/242344a0>.
- Grime, J. P. Evidence for the Existence of Three Primary Strategies in Plants and Its Relevance to Ecological and Evolutionary Theory. *The American Naturalist*, 111(982):1169–1194, 1977. ISSN 0003-0147. doi: 10.1086/283244.
- Hengge-Aronis, R. Survival of hunger and stress: The role of rpoS in early stationary phase gene regulation in *E. coli*. *Cell*, 72(2):165–168, 1 1993. ISSN 00928674. doi: 10.1016/0092-8674(93)90655-A. URL <https://linkinghub.elsevier.com/retrieve/pii/009286749390655A>.
- Himeoka, Y. and Mitarai, N. Dynamics of bacterial populations under the feast-famine cycles. *arXiv*, pages 1–39, 10 2019. URL <http://arxiv.org/abs/1910.05673>.
- Hoek, T. A., Axelrod, K., Biancalani, T., Yurtsev, E. A., Liu, J., and Gore, J. Resource Availability Modulates the Cooperative and Competitive Nature of a Microbial Cross-Feeding Mutualism. *PLOS Biology*, 14(8): e1002540, 8 2016. ISSN 1545-7885. doi: 10.1371/journal.pbio.1002540. URL <http://dx.plos.org/10.1371/journal.pbio.1002540>.

- Horsthemke, W. and Lefever, R. *Noise-Induced Transitions*, volume 15 of *Springer Series in Synergetics*. Springer Berlin Heidelberg, 2nd edition, 4 2006. ISBN 978-3-540-11359-1. doi: 10.1007/3-540-36852-3. URL <http://link.springer.com/10.1007/3-540-36852-3>.
- Hufton, P. G., Lin, Y. T., Galla, T., and McKane, A. J. Intrinsic noise in systems with switching environments. *Physical Review E*, 93(5):1–13, 2016. ISSN 24700053. doi: 10.1103/PhysRevE.93.052119.
- Jost, L. PARTITIONING DIVERSITY INTO INDEPENDENT ALPHA AND BETA COMPONENTS. *Ecology*, 88(10):2427–2439, 10 2007. ISSN 0012-9658. doi: 10.1890/06-1736.1. URL <http://doi.wiley.com/10.1890/06-1736.1>.
- Letten, A. D., Dhami, M. K., Ke, P. J., and Fukami, T. Species coexistence through simultaneous fluctuation-dependent mechanisms. *Proceedings of the National Academy of Sciences of the United States of America*, 115(26):6745–6750, 2018a. ISSN 10916490. doi: 10.1073/pnas.1801846115.
- Letten, A. D., Dhami, M. K., Ke, P. J., and Fukami, T. Species coexistence through simultaneous fluctuation-dependent mechanisms. *Proceedings of the National Academy of Sciences of the United States of America*, 115(26):6745–6750, 2018b. ISSN 10916490. doi: 10.1073/pnas.1801846115.
- Li, G., Xie, C., Lu, S., Nichols, R. G., Tian, Y., Li, L., Patel, D., Ma, Y., Brocker, C. N., Yan, T., Krausz, K. W., Xiang, R., Gavrilova, O., Patterson, A. D., and Gonzalez, F. J. Intermittent Fasting Promotes White Adipose Browning and Decreases Obesity by Shaping the Gut Microbiota. *Cell Metabolism*, 26(4):672–685, 2017. ISSN 19327420. doi: 10.1016/j.cmet.2017.08.019. URL <http://dx.doi.org/10.1016/j.cmet.2017.08.019>.
- Lin, Y. H., Bayrock, D. P., and Ingledew, W. M. Evaluation of *Saccharomyces cerevisiae* grown in a multistage chemostat environment under increasing levels of glucose. *Biotechnology Letters*, 24(6):449–453, 2002. doi: 10.1023/A:1014501125355.
- Mackey, R. L. and Currie, D. J. The diversity-disturbance relationship: Is it generally strong and peaked? *Ecology*, 82(12):3479–3492, 2001. ISSN 00129658. doi: 10.1890/0012-9658(2001)082[3479:TDDRII]2.0.CO;2.
- Merritt, J. and Kuehn, S. Frequency- and Amplitude-Dependent Microbial Population Dynamics during Cycles of Feast and Famine. *Physical Review Letters*, 121(9):098101, 8 2018. ISSN 0031-9007. doi: 10.1103/PhysRevLett.121.098101. URL <https://link.aps.org/doi/10.1103/PhysRevLett.121.098101>.
- Miller, A. D., Roxburgh, S. H., and Shea, K. How frequency and intensity shape diversity-disturbance relationships. *Proceedings of the National Academy of Sciences of the United States of America*, 108(14):5643–5648, 2011. ISSN 10916490. doi: 10.1073/pnas.1018594108.
- Mougi, A. and Kondoh, M. Diversity of Interaction Types and Ecological Community Stability. *Science*, 337(6092):349–351, 2012. ISSN 0036-8075. doi: 10.1126/science.1220529. URL <http://www.sciencemag.org/cgi/doi/10.1126/science.1220529>.

- Novick, A. and Szilard, L. Experiments with the Chemostat on Spontaneous Mutations of Bacteria. *Proceedings of the National Academy of Sciences*, 36(12):708–719, 12 1950. ISSN 0027-8424. doi: 10.1073/pnas.36.12.708. URL <http://www.pnas.org/cgi/doi/10.1073/pnas.36.12.708>.
- Novozhilov, A. S., Karev, G. P., and Koonin, E. V. Biological applications of the theory of birth-and-death processes. *Briefings in Bioinformatics*, 7(1):70–85, 3 2006. ISSN 1467-5463. doi: 10.1093/bib/bbk006. URL <https://academic.oup.com/bib/article/7/1/70/263777>.
- Piccardi, P., Vessman, B., and Mitri, S. Toxicity drives facilitation between 4 bacterial species. *Proceedings of the National Academy of Sciences*, 116(32):15979–15984, 2019. ISSN 0027-8424. doi: 10.1073/pnas.1906172116.
- Rodríguez-Verdugo, A., Vulin, C., and Ackermann, M. The rate of environmental fluctuations shapes ecological dynamics in a two-species microbial system. *Ecology Letters*, 22(5):838–846, 5 2019. ISSN 1461-023X. doi: 10.1111/ele.13241. URL <http://doi.wiley.com/10.1111/ele.13241>.
- Roesch, L. F., Fulthorpe, R. R., Riva, A., Casella, G., Hadwin, A. K., Kent, A. D., Daroub, S. H., Camargo, F. A., Farmerie, W. G., and Triplett, E. W. Pyrosequencing enumerates and contrasts soil microbial diversity. *ISME Journal*, 1(4):283–290, 2007. ISSN 17517362. doi: 10.1038/ismej.2007.53.
- Schreiber, S., Levine, J., Godoy, O., Kraft, N., and Hart, S. Does deterministic coexistence theory matter in a finite world? *bioRxiv*, 2020. doi: 10.1101/290882.
- Smits, S. A., Leach, J., Sonnenburg, E. D., Gonzalez, C. G., Lichtman, J. S., Reid, G., Knight, R., Manjurano, A., Changalucha, J., Elias, J. E., Dominguez-Bello, M. G., and Sonnenburg, J. L. Seasonal cycling in the gut microbiome of the Hadza hunter-gatherers of Tanzania. *Science*, 357(6353):802–805, 2017. ISSN 10959203. doi: 10.1126/science.aan4834.
- Srinivasan, S. and Kjelleberg, S. Cycles of famine and feast: The starvation and outgrowth strategies of a marine *Vibrio*. *Journal of Biosciences*, 23(4):501–511, 1998. ISSN 02505991. doi: 10.1007/BF02936144.
- Sun, Z., Koffel, T., Stump, S. M., Grimaud, G. M., and Klausmeier, C. A. Microbial cross-feeding promotes multiple stable states and species coexistence, but also susceptibility to cheaters. *Journal of Theoretical Biology*, 465:63–77, 2019. ISSN 00225193. doi: 10.1016/j.jtbi.2019.01.009. URL <https://linkinghub.elsevier.com/retrieve/pii/S0022519319300104>.
- Taitelbaum, A., West, R., Assaf, M., and Mobilia, M. Population Dynamics in a Changing Environment: Random versus Periodic Switching. *Physical Review Letters*, 125(4):048105, 7 2020. ISSN 0031-9007. doi: 10.1103/PhysRevLett.125.048105. URL <https://link.aps.org/doi/10.1103/PhysRevLett.125.048105>.
- Tecon, R., Mitri, S., Ciccarese, D., Or, D., van der Meer, J. R., and Johnson, D. R. Bridging the Holistic-Reductionist Divide in Microbial Ecology. *mSystems*, 4(1):17–21, 2019. ISSN 2379-5077. doi: 10.1128/mSystems.00265-18.

- Thaiss, C. A., Zeevi, D., Levy, M., Zilberman-Schapira, G., Suez, J., Tengeler, A. C., Abramson, L., Katz, M. N., Korem, T., Zmora, N., Kuperman, Y., Biton, I., Gilad, S., Harmelin, A., Shapiro, H., Halpern, Z., Segal, E., and Elinav, E. Transkingdom control of microbiota diurnal oscillations promotes metabolic homeostasis. *Cell*, 159(3):514–529, 2014. ISSN 10974172. doi: 10.1016/j.cell.2014.09.048. URL <http://dx.doi.org/10.1016/j.cell.2014.09.048>.
- Vasi, F., Travisano, M., and Lenski, R. E. Long-term experimental evolution in *Escherichia coli*. II. Changes in life-history traits during adaptation to a seasonal environment. *American Naturalist*, 144(3):432–456, 1994. ISSN 00030147. doi: 10.1086/285685. URL <https://www.jstor.org/stable/2462954>.
- West, R. and Mobilia, M. Fixation properties of rock-paper-scissors games in fluctuating populations. *Journal of Theoretical Biology*, 491:110135, 4 2020. ISSN 00225193. doi: 10.1016/j.jtbi.2019.110135. URL <http://dx.doi.org/10.1016/j.jtbi.2019.110135>.
- West, R., Mobilia, M., and Rucklidge, A. M. Survival behavior in the cyclic Lotka-Volterra model with a randomly switching reaction rate. *Physical Review E*, 97(2):022406, 2 2018. ISSN 2470-0045. doi: 10.1103/PhysRevE.97.022406. URL <https://link.aps.org/doi/10.1103/PhysRevE.97.022406>.
- Wienand, K., Frey, E., and Mobilia, M. Evolution of a Fluctuating Population in a Randomly Switching Environment. *Physical Review Letters*, 119(15):158301, 10 2017. ISSN 0031-9007. doi: 10.1103/PhysRevLett.119.158301. URL <https://link.aps.org/doi/10.1103/PhysRevLett.119.158301>.
- Wienand, K., Frey, E., and Mobilia, M. Eco-evolutionary dynamics of a population with randomly switching carrying capacity. *Journal of the Royal Society Interface*, 15(145):20180343, 8 2018. ISSN 17425662. doi: 10.1098/rsif.2018.0343. URL <https://royalsocietypublishing.org/doi/10.1098/rsif.2018.0343>.
- Xavier, J. B., Picioreanu, C., and Van Loosdrecht, M. C. M. A framework for multidimensional modelling of activity and structure of multispecies biofilms. *Environmental Microbiology*, 7(8):1085–1103, 2005. ISSN 14622912. doi: 10.1111/j.1462-2920.2005.00787.x.
- Zhao, Y. and Lin, Y. H. Growth of *Saccharomyces cerevisiae* in a chemostat under high glucose conditions. *Biotechnology Letters*, 25(14):1151–1154, 2003. ISSN 01415492. doi: 10.1023/A:1024577414157.
- Zuñiga, C., Li, C.-T., Yu, G., Al-Bassam, M. M., Li, T., Jiang, L., Zaramela, L. S., Guarnieri, M., Betenbaugh, M. J., and Zengler, K. Environmental stimuli drive a transition from cooperation to competition in synthetic phototrophic communities. *Nature Microbiology*, 4(12):2184–2191, 12 2019. ISSN 2058-5276. doi: 10.1038/s41564-019-0567-6. URL <http://www.nature.com/articles/s41564-019-0567-6>.

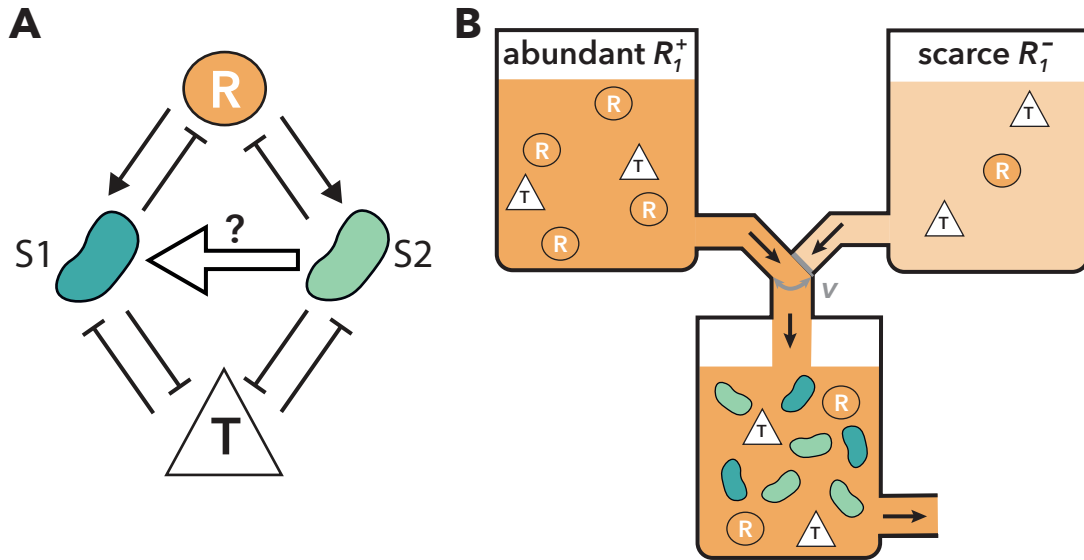


Figure 1: Schematic illustration of the model

A chemostat model with environmental switching. A: Interaction network when  $N = 2$ .  $A \rightarrow B$  represents that A increases B while  $A \dashv B$  represents that A decreases B. Two species compete for the same resource (R in a circle) but are killed by the same toxic compound (T in a triangle). As a proxy for species interactions, we follow the net effect of species 2 on species 1 (large arrow from species 2 to 1) – due to resource competition plus facilitation by detoxification – which can be environmentally mediated. B: An example of a chemostat model with environmental switching and  $N = 2$ . Environmental switching is realized by changing the media flowing into a chemostat. In this example, the current environmental condition is  $\xi = 1$  (abundant resource supply  $R_1^+$ ).

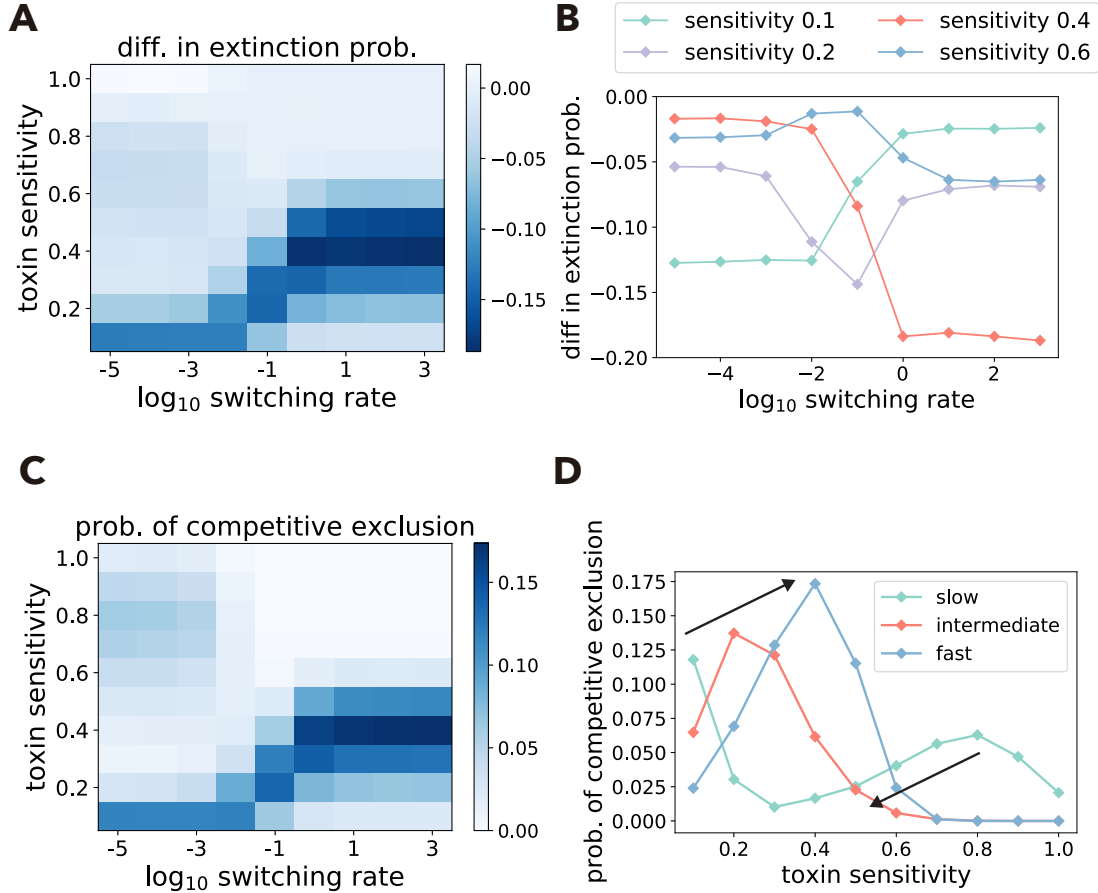


Figure 2: Species interaction strength changes differently over the switching rate

A: The effect of species 2 on species 1's extinction probability  $\Delta P(s_1(T_{end}) = 0)$  (Eq 7) changes over the switching rate  $\nu$  and the toxin sensitivity  $\delta = \delta_{11} = \delta_{21}$ . In most of the parameter space, species 2 has a negative effect on species 1.

B: Some illustrative examples from panel A plotted differently to show how  $\Delta P$  changes over the switching rate at given toxin sensitivities. The difference in extinction probability can monotonically increase ( $\delta = 0.1$ , green), monotonically decrease ( $\delta = 0.4$ , red), or non-monotonically change with a minimum ( $\delta = 0.2$ , purple) or a maximum ( $\delta = 0.6$ , blue) value at an intermediate switching rate.

C: Probability that species 2 persists but species 1 goes extinct (i.e., competitive exclusion) over switching rate and toxin sensitivity.

D: competitive exclusion probabilities over the toxin sensitivity, when the environmental switching rate is slow ( $\nu = 10^{-5}$ ), intermediate ( $\nu = 10^{-1}$ ), or fast ( $\nu = 10^3$ ).

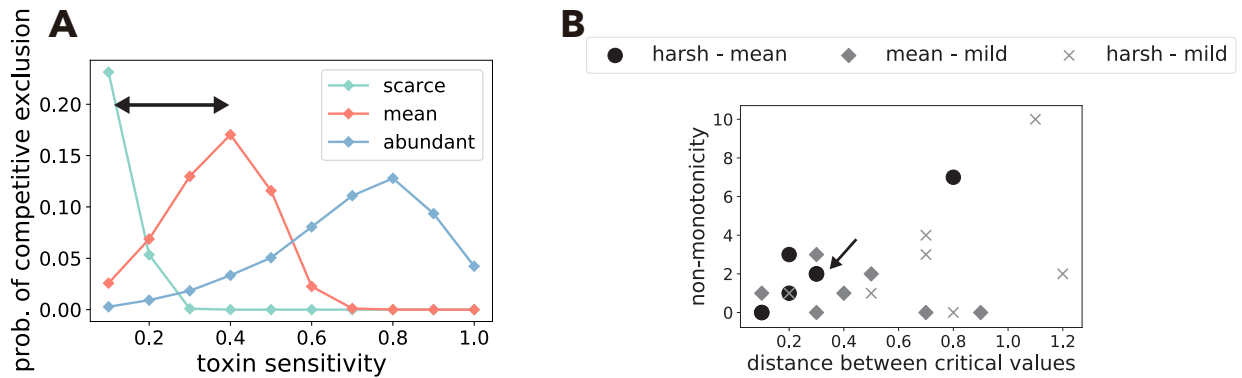


Figure 3: Competitive exclusion explains changes in species interactions

Analysis on competitive exclusion predicts at which toxin sensitivity the species interaction can change non-monotonically. A: In the absence of environmental switching, the competitive exclusion probability (i.e., probability that species 2 excludes species 1) is uni-modal over the switching rate. The toxin sensitivities giving the peak values (critical toxin sensitivities) depend on the resource supply: scarce  $R_1 = R_1^-$  (green), mean  $R_1 = \langle R_1 \rangle$  (red), or abundant  $R_1 = R_1^+$  (blue). B: The number of times we observe non-monotonic species interactions across the explored parameter range changes with the distance between the two critical toxin sensitivities, depending on where distances are measured (between harsh and mean environments: dots, between mean and mild: environment diamonds, and between harsh and mild environments: crosses). These three distances were measured in each of the following seven scenarios: three different scenarios of environmental switching (Table 1 and Appendix 4) and four environmental switching scenario 1s with changing amounts of resource supplies (Appendix 5). The correlation is only significantly positive for the distance between scarce resource or abundant toxin supplies (i.e., harsh environments) and mean resource/toxin supplies (Spearman's  $\rho = 0.77$ , P-value: 0.043). The distance corresponding to the scenario analyzed in the main text is shown by the black arrow in panel A, where scarce resources are considered to be a harsh environment (dot indicated by the arrow in panel B).

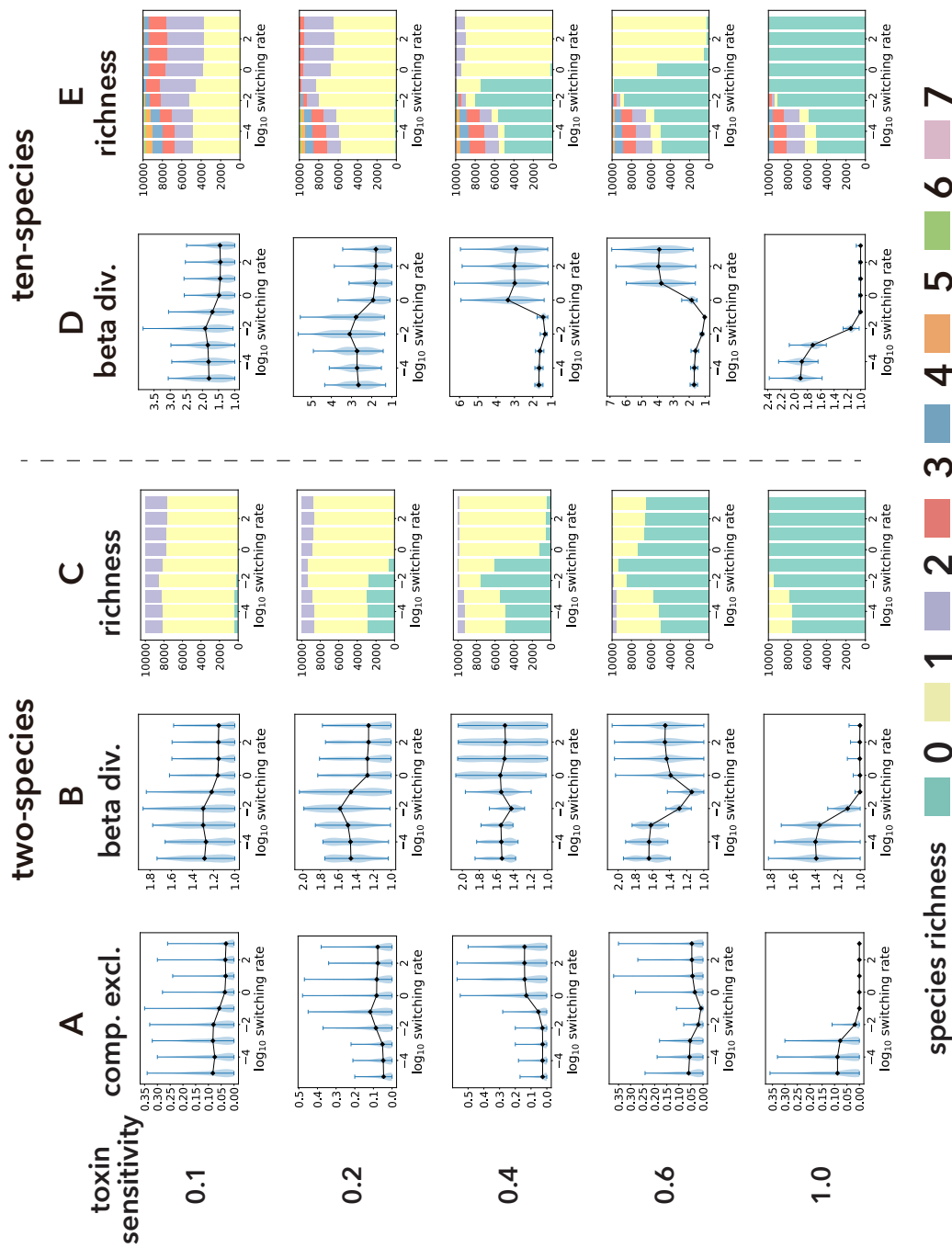


Figure 4: Comparison of competitive exclusion and beta diversity

Competitive exclusion probabilities (column A), beta diversities (column B), and species richness (column C) over the switching rate in two-species communities. Here, competitive exclusion refers the event where the slower-growing species excludes the faster-growing species. Columns D and E show the beta diversity and species richness in ten-species communities, respectively. In the plots of competitive exclusion probability and beta diversity, the black lines show the means and blue areas represent the probability distributions calculated from 10'000 simulations (100 beta diversity and each of them from 100 replicate runs). Each color in the species richness plots represents the proportion of 10'000 runs where at the end of the run there were that number of species surviving. Each row represents the mean toxin sensitivity  $\bar{\delta}$  of communities in those runs.



Table 1: Different scenarios of environmental switching

| Scenario | $R_i(\xi = 1)$        | $R_i(\xi = -1)$       | $T_j(\xi = 1)$        | $T_j(\xi = -1)$       |
|----------|-----------------------|-----------------------|-----------------------|-----------------------|
| 1        | $R_i^+$               | $R_i^-$               | $\langle T_j \rangle$ | $\langle T_j \rangle$ |
| 2        | $\langle R_i \rangle$ | $\langle R_i \rangle$ | $T_j^-$               | $T_j^+$               |
| 3        | $R_i^+$               | $R_i^-$               | $T_j^-$               | $T_j^+$               |

## Supplementary information

### Appendix 1 Analysis excluding noise

In this section, we analyse the equilibrium state of a two-species, one-resource, and one-toxin model, neglecting environmental switching and demographic noise. Although an equilibrium state cannot be analytically obtained, we shall see that there exists at most one stable and feasible (species abundance  $s_k > 0$ ) equilibrium state. By neglecting demographic noise and environmental switching from Eq (5) in the main text, the dynamics are governed by the following ordinary differential equations:

$$\dot{r}_1 = \alpha (R_1 - r_1) - \sum_{k=1,2} \frac{\mu_{1k}}{Y_{1k}^r} \frac{r_1}{r_1 + K_{1k}^r} s_k, \quad (\text{A.1a})$$

$$\dot{t}_1 = \alpha (T_1 - t_1) - \sum_{k=1,2} \frac{\delta_{1k}}{Y_{1k}^t} \frac{t_1}{t_1 + K_{1k}^t} s_k, \quad (\text{A.1b})$$

$$\dot{s}_k = \left( \mu_{1k} \frac{r_1}{r_1 + K_{1k}^r} - \delta_{1k} \frac{t_1}{t_1 + K_{1k}^t} - \alpha \right) s_k, \quad (\text{A.1c})$$

When only species  $k$  persists in the system, a feasible<sup>1</sup> equilibrium state of Eqs (A.1a) -(A.1c),  $(r_1, t_1, s_k) = (r_{1k}^*, t_{1k}^*, s_k^*)$ , should satisfy below:

$$\alpha (R_1 - r_{1k}^*) = \frac{\mu_{1k}}{Y_{1k}^r} \frac{r_{1k}^*}{r_{1k}^* + K_{1k}^r} s_k^*, \quad (\text{A.2a})$$

$$\alpha (T_1 - t_{1k}^*) = \delta_{1k} Y_{1k}^t \frac{t_{1k}^*}{t_{1k}^* + K_{1k}^t} s_k^*, \quad (\text{A.2b})$$

$$\mu_{1k} \frac{r_{1k}^*}{r_{1k}^* + K_{1k}^r} = \delta_{1k} \frac{t_{1k}^*}{t_{1k}^* + K_{1k}^t} + \alpha. \quad (\text{A.2c})$$

By rearranging the first and second equations, we see that they represent quadratic functions of  $r_{1k}^*$  and  $t_{1k}^*$ :

$$-r_{1k}^{*2} + \{R_1 - K_{1k}^r - \mu_{1k} s_k^*/(\alpha Y_{1k}^r)\} r_{1k}^* + K_{1k}^r R_1 = 0, \quad (\text{A.3})$$

$$-t_{1k}^{*2} + \{T_1 - K_{1k}^t - \delta_{1k} s_k^*/(\alpha Y_{1k}^t)\} t_{1k}^* + K_{1k}^t T_1 = 0. \quad (\text{A.4})$$

Notice that  $K_{1k}^r R_1$  and  $K_{1k}^t T_1$  are positive. This implies that the above equations always have a unique positive root. In other words, we can obtain unique solutions for  $r_{1k}^*$  and  $t_{1k}^*$  once we obtain  $s_k^*$ .

By substituting the positive roots of Eqs (A.3) and (A.4) into Eq (A.2c), we obtain the following equation whose positive root is  $s_k^*$ :

$$f(s) = \frac{1}{2\alpha} \left\{ (-\mu_{1k} + 2\alpha + \delta_{1k}) s + \sqrt{Q_1(s)} - \sqrt{Q_2(s)} + \alpha (-K_{1k}^r Y_{1k}^r + K_{1k}^t Y_{1k}^t - Y_{1k}^r R_1 + Y_{1k}^t T_1) \right\} \quad (\text{A.5})$$

---

<sup>1</sup>Here, feasibility means  $r_{1k}^*, t_{1k}^*, s_k^* > 0$

where  $Q_1(s)$  and  $Q_2(s)$  are quadratic functions of  $s$ :

$$Q_1(s) = \{\mu_{1k}s + \alpha Y_{1k}^r (K_{1k}^r - R_1)\}^2 + 4\alpha Y_{1k}^r K_{1k}^r R_1 > 0 \quad (\text{A.6a})$$

$$Q_2(s) = \{\delta_{1k}s + \alpha Y_{1k}^t (K_{1k}^t - T_1)\}^2 + 4\alpha Y_{1k}^t K_{1k}^t T_1 > 0. \quad (\text{A.6b})$$

Notice that  $f(s)$  always has a root  $s = 0$  because

$$\begin{aligned} f(0) &= \frac{1}{2\alpha} \left\{ \sqrt{Q_1(0)} - \sqrt{Q_2(0)} + \alpha (-K_{1k}^r Y_{1k}^r + K_{1k}^t Y_{1k}^t - Y_{1k}^r R_1 + Y_{1k}^t T_1) \right\} \\ &= \frac{1}{2\alpha} \left\{ \alpha Y_{1k}^r (K_{1k}^r + R_1) - \alpha Y_{1k}^t (K_{1k}^t + T_1) + \alpha (-K_{1k}^r Y_{1k}^r + K_{1k}^t Y_{1k}^t - Y_{1k}^r T_1 + Y_{1k}^t T_1) \right\} \\ &= 0. \end{aligned} \quad (\text{A.7})$$

Although Newton's method numerically provides a root of  $f(s)$ , this root depends on the initial value used in Newton's method. In addition, as  $f(s)$  has root  $s = 0$ , Newton's method may provide this root with various initial values, which does not always mean that  $f(s)$  does not have positive roots (i.e.,  $s_k^*$ ). In other words, it is recommended to investigate how many positive roots  $f(s)$  has before using Newton's method.

To investigate the number of  $f(s)$ 's positive roots, it is useful to obtain  $df/ds$ :

$$\frac{df}{ds} = \frac{1}{2\alpha} \left\{ (-\mu_{1k} + 2\alpha + \delta_{1k}) + \frac{dQ_1/ds}{2\sqrt{Q_1(s)}} - \frac{dQ_2/ds}{2\sqrt{Q_2(s)}} \right\}. \quad (\text{A.8})$$

Although it is analytically difficult to obtain the solution(s) of  $df/ds$ , we can obtain the maximum number of positive roots of  $f(s)$  by analyzing the number of  $df/ds$ 's sign changes. Notice that  $dQ_1/ds$  and  $dQ_2/ds$  are linear functions of  $s$ :

$$\frac{dQ_1}{ds} = 2\mu_{1k} \{\mu_{1k}s + \alpha Y_{1k}^r (K_{1k}^r - R_1)\}, \quad (\text{A.9a})$$

$$\frac{dQ_2}{ds} = 2\delta_{1k} \{\delta_{1k}s + \alpha Y_{1k}^t (K_{1k}^t - T_1)\}. \quad (\text{A.9b})$$

In addition,  $Q_1(s)$  and  $Q_2(s)$  are always positive. Then, the second and third terms of Eq (A.8) change their sign at most once by increasing  $s$ . The maximum number of  $df/ds$ 's sign change is, therefore, two. This implies that the maximum number of positive roots of  $f(s)$  is also two. To obtain the exact number of positive roots of  $f(s)$ , it is necessary to numerically calculate the root(s) of  $df/ds$ . Substituting the root(s) into Eq (A.5) and calculating the sign of  $f(s)$ , it is possible to obtain the exact value of  $s_k^*$ .

Once we have obtained a feasible equilibrium state  $(r_{1k}^*, s_k^*, t_{1k}^*)$ , it is necessary to analyze the stability of this equilibrium state. Although the stability analysis requires the evaluation of the Jacobian matrix at each equilibrium state, we can see that there exists at most one feasible and stable equilibrium state without such

stability analysis. Notice that:

$$\begin{aligned}
& \dot{s}_j \leq 0 \\
\Leftrightarrow & \mu_{1k} \frac{r_{1k}^*}{r_{1k}^* + K_{1k}^r} \leq \delta_{1k} \frac{t_{1k}^*}{t_{1k}^* + K_{1k}^t} + \alpha \\
\Leftrightarrow & f(s) \geq 0.
\end{aligned} \tag{A.10}$$

These inequalities implies that a stable equilibrium state satisfies the following inequality:

$$\left. \frac{df}{ds} \right|_{s=s_k^*} > 0. \tag{A.11}$$

Although there can exist at most two feasible equilibria, only one of them satisfies the above inequality (Fig. A.1). The number of feasible and stable equilibria is, therefore, one at most.

## Appendix 2 Details of simulations

### Appendix 2.1 Species interaction analysis

Here, we summarize the details of the simulations and parameter values used for species interaction analysis in the main text. In the analysis of species interactions, we used the minimal model ( $N = 2$ ): two species compete for one resource and absorb and are killed by one toxin. As the model represents a stochastic process in a continuous-time scale, the simulation is implemented by the Gillespie algorithm (Gillespie, 1977). In each run, the initial condition is either  $(r_1(0), t_1(0), s_1(0), s_2(0)) = (150, 100, 10, 0)$  or  $(150, 100, 10, 10)$ , where species 2 is absent or present, respectively. The initial environmental condition is  $\xi = 1$  with a probability of 0.5; otherwise  $\xi = -1$ . Each simulation continues until at time  $T_{end} = 200$  when the distributions of species abundances converge to a quasi-stationary distribution and do not change for a long time. The extinction probability is estimated by running  $10^5$  simulations for each condition.

Table A.1 summarizes the parameter values used in the species interaction analysis. In the main text, species 2 is assumed to grow slower than species 1, meaning that species 2 goes extinct in the absence of demographic noise. For simplicity, we assumed that species 2's parameter values are the same as those of species 1 except for the maximum growth rate.

In the main text, to investigate how species 2's effect on species 1 changes over the switching rate, we began by analyzing the difference in the extinction probability of species 1 in the presence/absence of species 2 as a proxy for species interactions, but then moved to using the competitive exclusion probability instead. Although Fig. 2A and C shows that these two measures give similar results, Fig. A.2 confirms this conclusion as the ratio of these two measures is around 1.

## Appendix 2.2 Species diversity analysis

In the community diversity analysis, we changed the number of species from  $N = 2$  to  $N = 10$ . Some parameter values were not fixed in this analysis, and we sampled them from the following probability density functions:

$$\mu_{ik} \sim \mathcal{N}(1, 0.1^2), \quad (\text{A.12a})$$

$$\delta_{jk} \sim \text{Beta}(100\bar{\delta}, 100(1 - \bar{\delta})), \quad (\text{A.12b})$$

$$K_{ik}^r, K_{jk}^t \sim \mathcal{N}(100, 10^2). \quad (\text{A.12c})$$

Here, each function is uni-modal with a mean of 1.0 for  $\mu_{ik}$ ,  $\bar{\delta}$  for  $\delta_{jk}$ , and 100 for  $K_{ik}^r, K_{jk}^t$ . For  $\mu_{ik}, K_{ik}^r$ , and  $K_{jk}^t$ , the mean values are the same as in Table A.1 and they are rarely negative due to the small variances. We sampled  $\delta_{jk}$  from a beta distribution so that  $0 \leq \delta_{jk} \leq 1$ :  $\delta_{jk}$  should be non-negative by definition and not be larger than 1 because a large  $\delta_{jk}$  is likely to drive species  $k$  extinct. We systematically vary the value of the mean toxin sensitivity  $\bar{\delta}$  to be  $\bar{\delta} = 0.1, 0.2, 0.4, 0.6$  or  $0.99$  in each set of simulations. We used  $\bar{\delta} = 0.99$  instead of  $\bar{\delta} = 1.0$  because the beta distribution did not generate different values of  $\delta_{jk}$  with  $\bar{\delta} = 1.0$ . For each number of species  $N$  (2, 4, 6, 8 or 10) and  $\bar{\delta}$ , 100 sets of parameter values are sampled. With each parameter set, we performed the simulation 100 times until  $T_{end} = 200$  at each value of the environmental switching rate  $\nu$ . Then, we calculated the species richness and beta diversity as described in the main text.

In each run, initial resource amounts, species abundances, and toxin amounts are given by  $(r_i(0), t_j(0), s_k(0)) = (150, 150, 10)$  for any  $i, j, k$ . As an environmental switching scenario, we chose scenario 1 (Table 1) with  $R_i^+ = 200$ ,  $R_i^- = 50$ , and  $\langle T_k \rangle = 125$  for any  $i$  and  $k$ . The initial environmental condition is  $\xi = 1$  with probability of 0.5; otherwise  $\xi = -1$ .

## Appendix 3 Analysis in the absence of environmental switching

The analysis with an environmental switching rate of 0 facilitates the understanding of the results in the two extreme switching rates ( $\nu \rightarrow 0$  and  $\nu \rightarrow \infty$ ) in the main text. In this section, we analyze species 2's effect on species 1 when the resource supply is fixed to be scarce, mean, or abundant.

In the absence of environmental switching, resource supply and toxin sensitivity change species 2's effect on species 1 (Fig. A.3): each resource supply has a unique maximum negative interaction, which is reached at a certain toxin sensitivity. These toxin sensitivities correspond to the peak sensitivities of competitive exclusion probabilities (Fig. 3A). Species 2's effect on species 1 converges to zero when the toxin sensitivities exceed the peak sensitivities as competitive exclusion probabilities decrease (see section 3.3). This is because both species 1 and species 2 go extinct at too high toxin sensitivity (Fig. A.4).

Note that species 2 has a positive effect on species 1 when the resource supply is abundant and toxin sensitivity is 1.0. In this case, the benefits of absorbing toxic compounds by species 2 overcome the costs of competing for the resource. This is why in Fig. 2A, species 2 has a positive effect on species 1 when the switching rate is very small ( $\nu \leq 10^{-3}$ ) and the toxin sensitivity is 1.0.

## Appendix 4 Alternative environmental switching scenarios

In the main text, environmental switching affects only the resource supply (scenario 1) while the amount of toxin supply is fixed. Here, the results of other environmental switching scenarios are shown: In scenario 2, environmental switching affects only the toxin supply, while both resource and toxin supplies change and correlate negatively in scenario 3 (see Table 1).

In both scenarios 2 and 3, the difference in species 1's extinction probability  $\Delta P(s_1(T_{end}) = 0)$  is very similar to the negative competitive exclusion probability when the sign of  $\Delta P(s_1(T_{end}) = 0)$  is negative (Fig. A.5). This once again confirms that we can use one measure or the other.

In addition, in both scenarios, the probabilities of competitive exclusion are bi-modal across toxin sensitivities at very slow environmental switching  $\nu = 10^{-5}$ , but uni-modal at very fast environmental switching ( $\nu = 10^3$ ) (Fig. A.5C, D). As explained in the main text, when  $\nu \rightarrow 0$ , there are no switches and the environmental state is randomly allocated to harsh or mild conditions at  $t = 0$  with the same probability (the mean of  $\xi$  is zero), yielding a bi-modal distribution at low switching rate. In the limit  $\nu \rightarrow \infty$ , there are so many switches that environmental noise averages out, i.e.  $\xi$  is replaced by its mean (that is zero). This results in a uni-modal distribution when  $\nu \gg 1$ .

Whether or not we observe non-monotonic effects of environmental switching differs in the two scenarios. In scenario 2, we do not observe any non-monotonic effects (Fig. A.5C). This is because the critical toxin sensitivity under abundant toxin supply ( $\delta = 0.3$ ) is close to that under mean toxin supply ( $\delta = 0.4$ ). In contrast, we do observe non-monotonic effects of environmental switching rate in scenario 3 (Fig. A.5D): when  $\delta = 0.2$ , an intermediate switching rate ( $\nu = 10^{-1}$ ) shows the minimum difference in extinction probability, and the maximum probability of competitive exclusion. Although in scenario 3 the same intermediate switching rate minimizes the probability of competitive exclusion at  $\delta = 0.6$ , the same non-monotonic effect is not observed in the difference in extinction probabilities (Fig. A.5B). Note that the critical toxin sensitivities under the mild environments in scenarios 2 (scarce toxin supply) and 3 (abundant resource supply and scarce toxin supply) are slightly larger than 1.0 (Fig. A.6) and therefore not visible in Fig. A.5D. Table A.2 shows the critical toxin sensitivities in each scenario.

## Appendix 5 Effects of resource supply

In this section, we again focus on environmental switching scenario 1 (changing only resource supply). We will see that the amount of resource supplies  $R_1(\xi)$  changes the critical toxin sensitivities under scarce, mean, and abundant, resource supplies, affecting the likelihood of the non-monotonic effect of the environmental switching rate.

By increasing the abundant or decreasing the scarce resource supply (Figs. A.7A and D, respectively), the distance between the critical toxin sensitivities under scarce and mean (or mean and abundant) resource supplies becomes larger (Table A.2). Conversely, decreasing abundant or increasing scarce resource supply (Figs. A.7B

and C, respectively), decreases the distance between the critical toxin sensitivities under scarce and mean (or mean and abundant) resource supplies (Table A.2). Once again, changes in competitive exclusion probability (A.7) match changes in species 2's effect on species 1 (Fig. A.8).

Analyzing competitive exclusion probability instead of the difference in extinction probability is valid only when the difference in extinction probability is negative: if it is positive, the second line in (11) cannot be ignored. The sign of the difference can, however, become positive at  $\delta = 1.0$ . Indeed, when  $R_1^+ = 400$  and  $\delta = 1.0$ , species 2 has a positive effect on species 1 whose strength varies non-monotonically with the rate of environmental switching (A.9A). In this case, we analyze both (i) the competitive exclusion probability (the first line in Eq (11), Fig. A.9B) and (ii) the difference in species 1's extinction probability in mono-culture and both species extinction in co-culture (the second line in Eq (11), Fig. A.9C). The effects of the environmental switching rate on (i) and (ii) are similar, leading to similar non-monotonic effects of species 2 on species 1. In sum, non-monotonic effects of environmental switching rates on species interactions can be observed whether these interactions are positive or negative. Although the main text explains why non-monotonic effects of environmental switching rates on species interactions happen when interactions are negative, it remains unclear why such non-monotonic changes happen when species interactions are positive.

## Appendix 6 Diversity in communities of increasing species number

In the main text, we show the distributions of beta diversity and species richness in communities when the initial number of species  $N$  is two or ten. This section shows the results of intermediates values of  $N = 4, 6, 8$ . The number of initial species does not change how beta diversity changes over the environmental switching rate, except when the mean toxin sensitivity  $\bar{\delta} = 0.4$  (Fig. A.10). These results indicate that beta diversity and the probability of competitive exclusion change similarly over the switching rate when the initial number of species is larger than two.

The initial number of species  $N$  in a community affects the maximum values of species richness (Fig. A.11). However, how the switching rate and the mean toxin sensitivity affect the distribution of species richness was consistent for different values of  $N$ . In particular, increasing the mean toxin sensitivity decreases species richness. The effects of the environmental switching rate also depend on the mean toxin sensitivity: at mean toxin sensitivity 1.0, species in all community sizes are more likely to go extinct as the switching rate increases, while the likelihood of all species going extinct consistently shows a humped shape at toxin sensitivity 0.4 or 0.6.

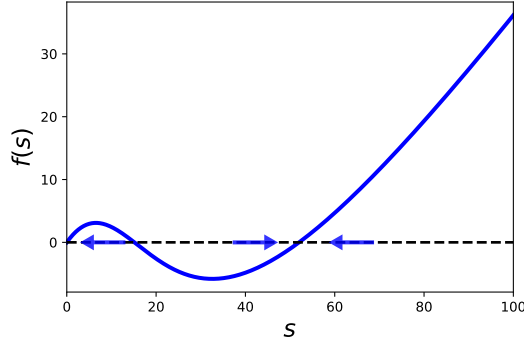


Figure A.1: Feasible and stable equilibrium state

An example of  $f(s)$  and equilibrium states. In this example,  $f(s)$  has three roots:  $s = 0$ , and two feasible equilibria. The blue arrows indicate that  $s$  decreases or increases when  $f(s)$  is positive or negative, respectively. As  $df/ds$  is negative at the smaller feasible equilibrium state, this equilibrium state is unstable. On the other hand, the larger feasible equilibrium has a positive  $df/ds$ . Note that the equilibrium state corresponding to  $s = 0$  can be also stable. Parameter values are  $\delta_{1k} = 1.2$ ,  $R_1 = 200$ ,  $T_1 = 125$  and as in Table A.1 otherwise.

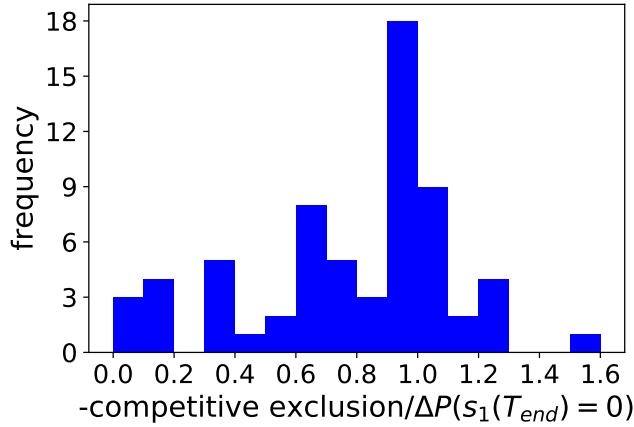


Figure A.2: Competitive exclusion probability relative to the difference in extinction probability of species 1 in the presence/absence of species 2

A histogram of the ratio of the competitive exclusion probability and the difference in species 1's extinction probabilities alone versus in the presence of species 1, showing the results of 81 sets of the environmental switching rate  $\nu$  and the toxin sensitivity  $\delta$  (9 values of  $\nu = 10^{-5}, \dots, 10^3$  and 9 values of  $\delta = 0.1, \dots, 0.9$ ). For each set of the parameter values,  $10^5$  simulations were run to calculate the competitive exclusion probability and the difference in species 1's extinction probabilities in the presence/absence of species 2. In many of these 81 parameter sets, this ratio is close to 1, indicating that both measures yield similar results. As in the manuscript we focus on conditions leading to competition between the two species, we ignore toxin sensitivity  $\delta = 1.0$  where species 2's effect on species 1 can be positive.



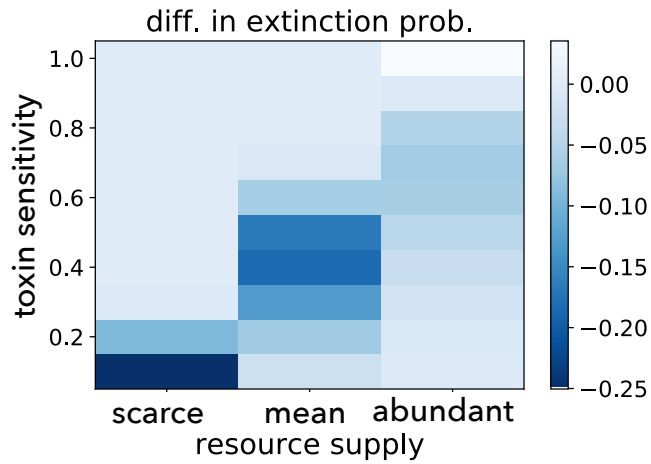


Figure A.3: Species 2's effect on species 1 in the absence of environmental switching

Species 2's effect on species 1 when the resource supply is fixed to be scarce ( $R_1^-$ ), mean ( $\langle R_1 \rangle$ ), or abundant ( $R_1^+$ ). The toxin sensitivities that minimize species 2's effect on species 1 correspond to the peak sensitivities in Fig. 3A.

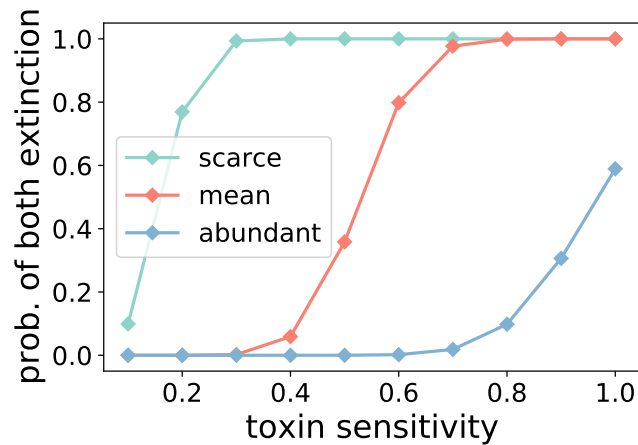


Figure A.4: Probability of both species going extinct in the absence of environmental switching

Probabilities that both species 1 and species 2 go extinct when resource supply is fixed to be scarce ( $R_1^-$ ), mean ( $\langle R_1 \rangle$ ), or abundant ( $R_1^+$ ).

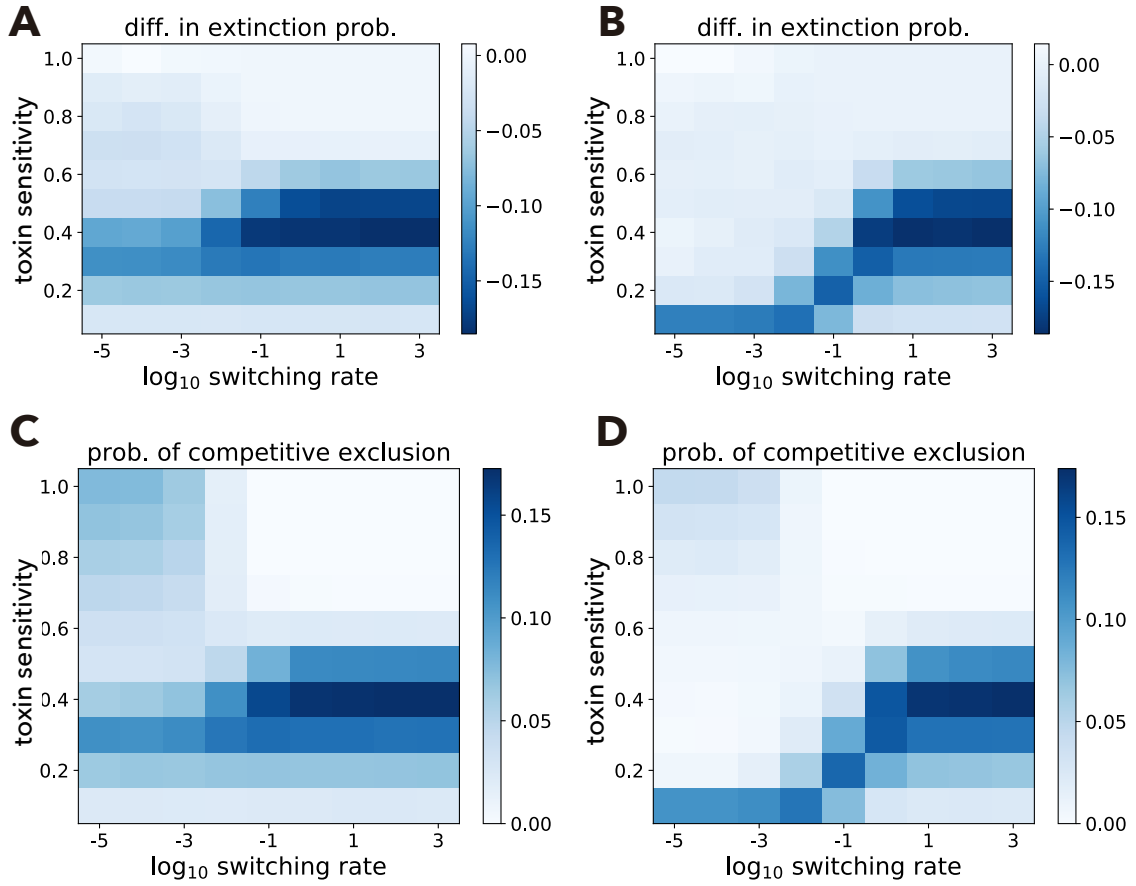


Figure A.5: Effects of the environmental switching rate in alternative scenarios

Examples of the effect of switching rate in alternative scenarios. In the left column (A and C), toxin supply is switching (scenario 2), while both resource and toxin supplies switch and are negatively correlated (scenario 3) in the right column (B, D). A and B: difference between extinction probabilities in absence and presence of species 2. C and D: competitive exclusion probability. Parameter values:  $R_1^+ = 200$ ,  $R_1^- = 50$ ,  $T_1^+ = 200$ , and  $T_1^- = 50$ .

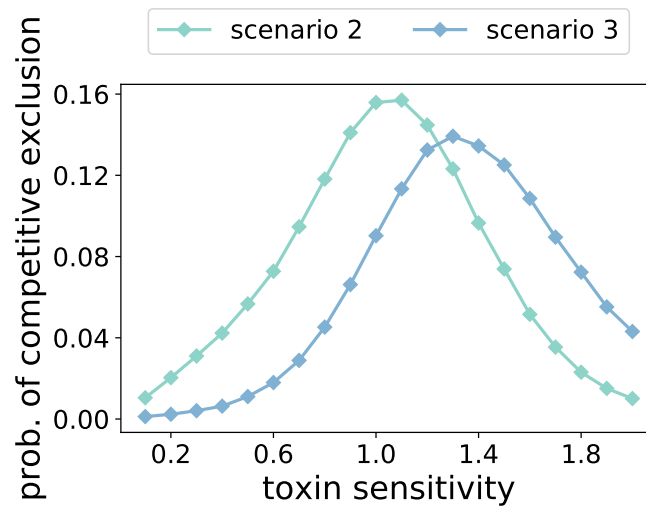


Figure A.6: Critical toxin sensitivities under mild environments

The critical toxin sensitivities (i.e., toxin sensitivity that maximizes the competitive exclusion probability in the absence of environmental switching) under the mild environments (scenario 2 :scarce toxin supply  $T_1^- = 50$ , and scenario 3: abundant resource supply  $R_1^+ = 200$  and scarce toxin supply) are  $> 1$ .

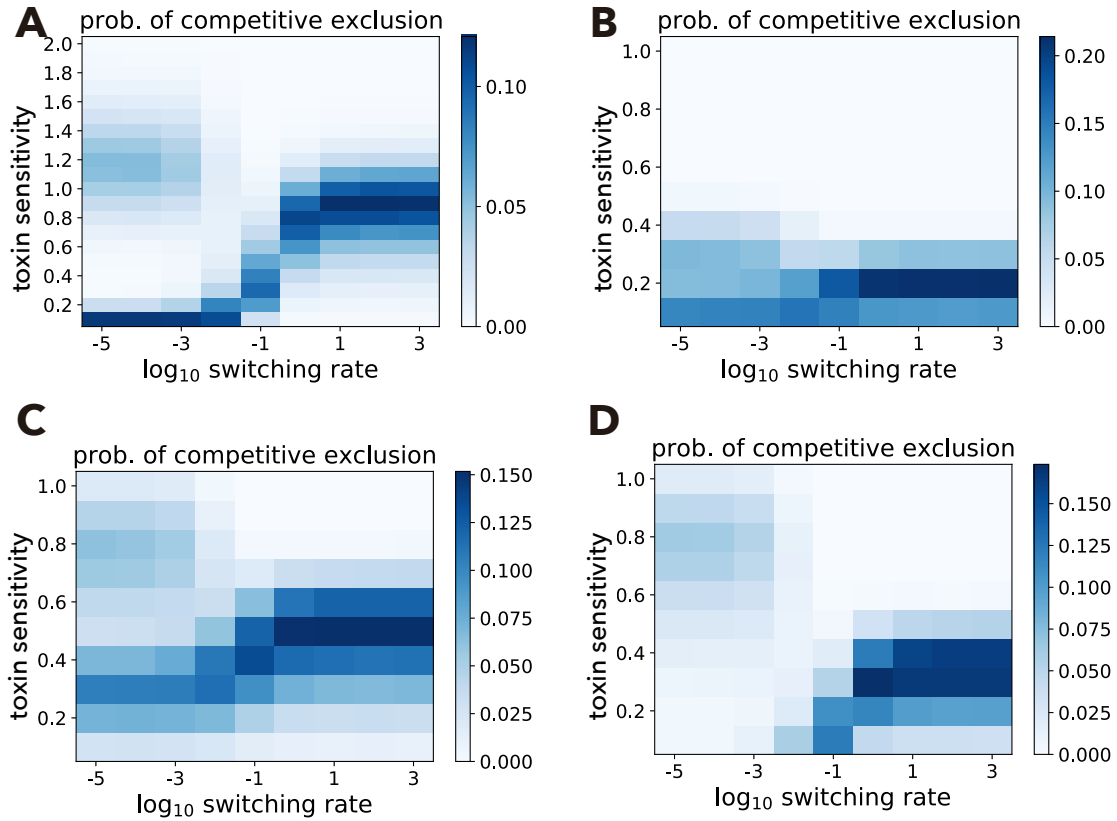


Figure A.7: Effects of resource supplies on competitive exclusion

Top: abundant resource supply becomes twice (A) or half (B) of  $R_1^+ = 200$ , i.e.  $R_1^+ = 400$  in panel (A) and  $R_1^+ = 100$  in panel (B). Bottom: scarce resource supply becomes twice (C) or half (D) of  $R_1^- = 50$ , i.e.  $R_1^- = 100$  in panel (C) and  $R_1^- = 25$  in panel (D).

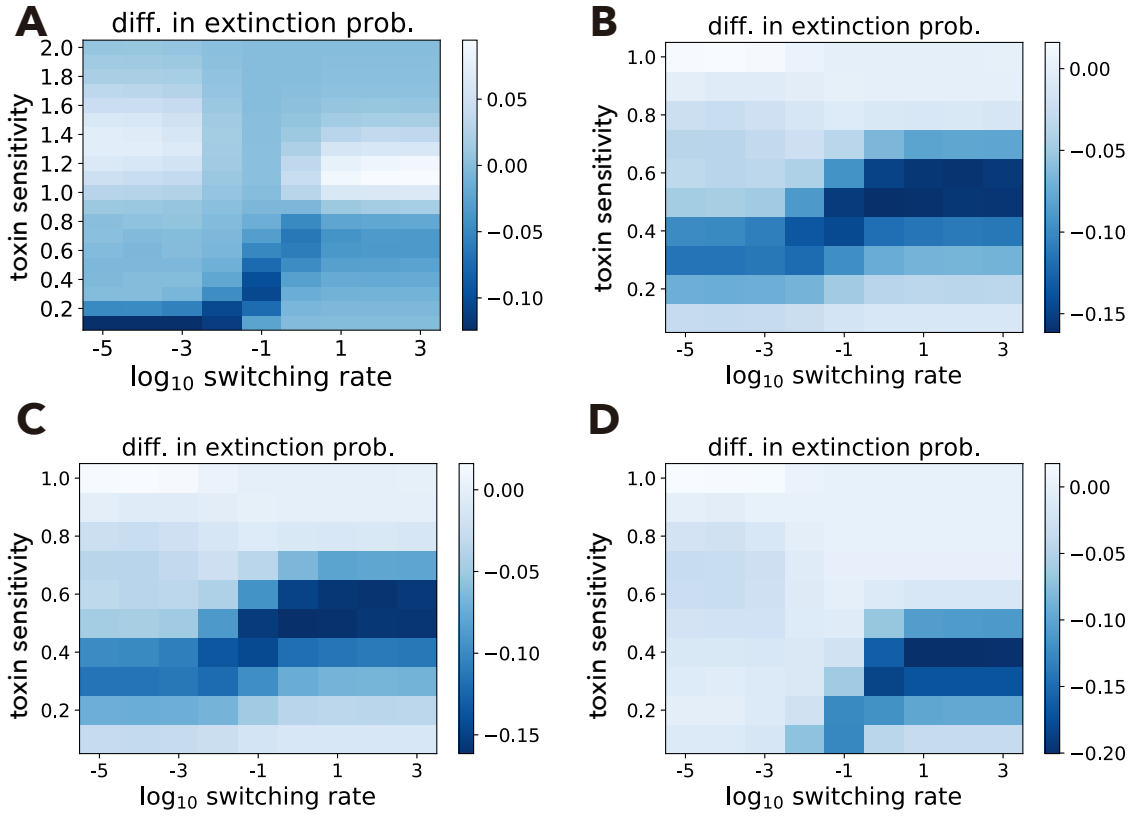


Figure A.8: Effects of resource supplies on species interactions

Similar to Fig. A.7 but showing species 2's effect on species 1's extinction probability. Top: abundant resource supply becomes twice (A) or half (B) of  $R_1^+ = 200$ , i.e.  $R_1^+ = 400$  in panel (A) and  $R_1^+ = 100$  in panel (B). Bottom: the scarce resource supply becomes twice (C) or half (D) of  $R_1^- = 50$ , i.e.  $R_1^- = 100$  in panel (C) and  $R_1^- = 25$  in panel (D). We plotted toxin sensitivity from 0.1 to 2.0 in panel A to see non-monotonic positive species interactions (see also Fig.A.9)

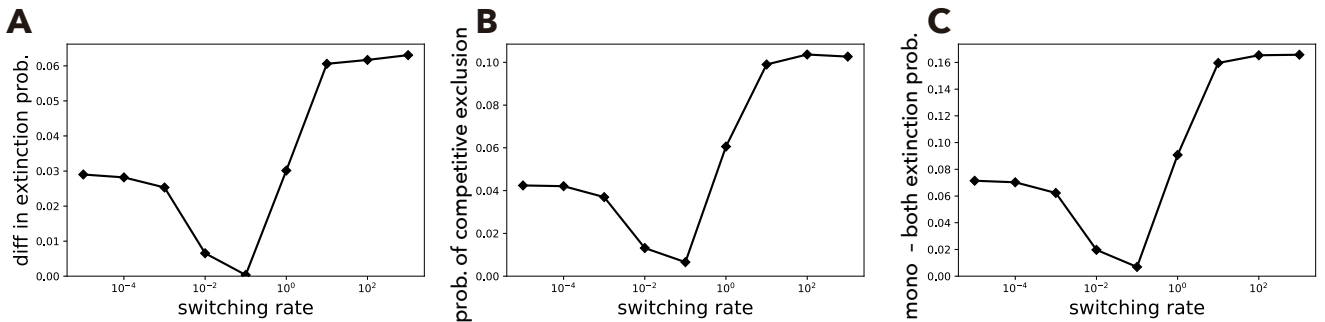


Figure A.9: Positive interaction strength varies non-monotonically with switching rate

A: Difference in species 1's extinction probability with positive sign at  $\delta = 1.0$  and  $R_1^+ = 400$ , showing a non-monotonic effect of the environmental switching rate. B: Probability of competitive exclusion. C: Difference between the probability of species 1 going extinct alone and both species going extinct. Parameter values are  $s^+ = 400$ ,  $\delta = 1.0$ .

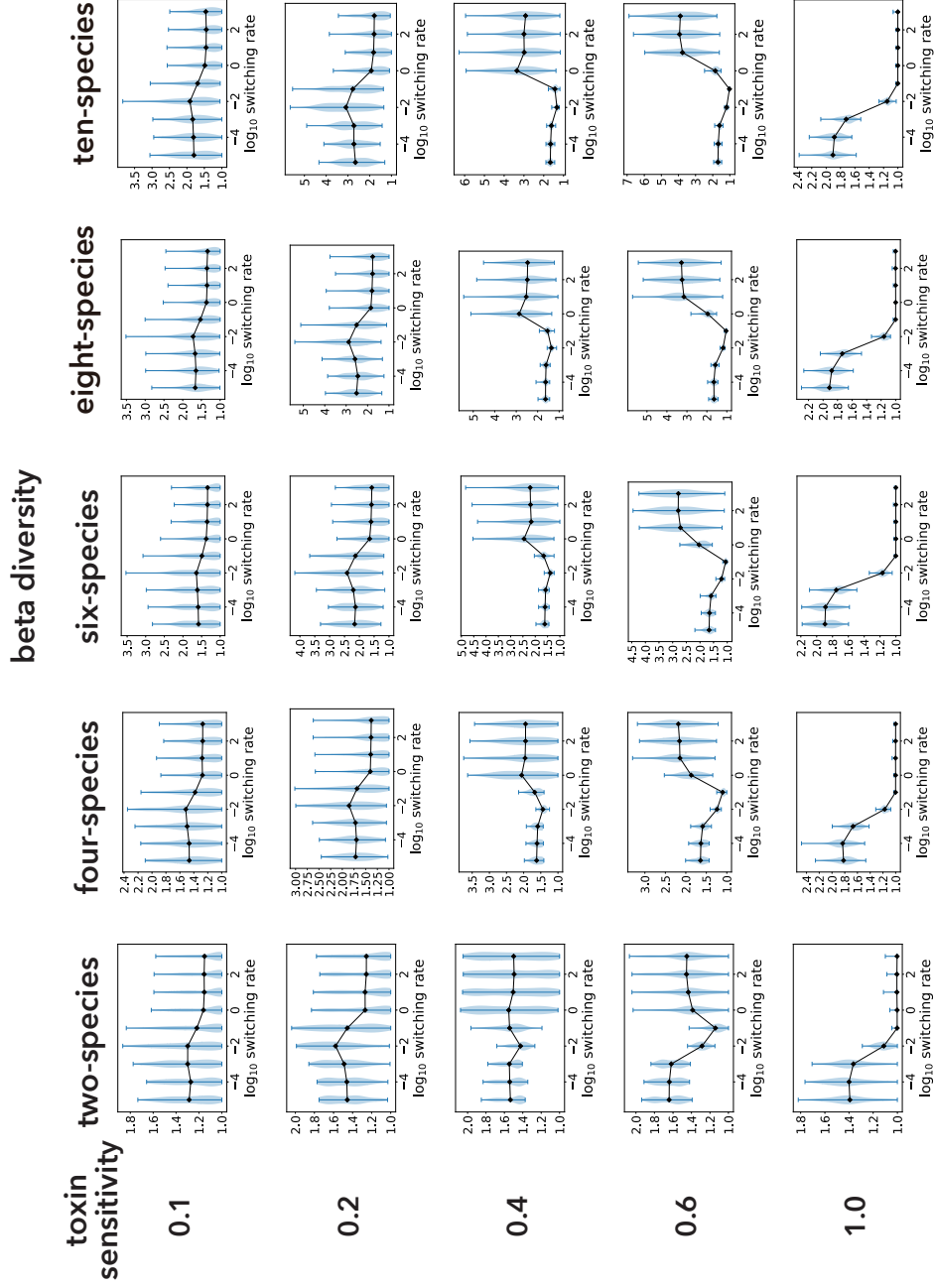


Figure A.10: Beta diversity with increasing initial number of species in a community

Beta diversities with increasing initial numbers of species  $N$  and mean toxin sensitivities  $\bar{\delta}$ . The black lines show the means and blue areas represent the probability distributions calculated by 10'000 simulations (100 beta diversity measurements using different parameter sets, each from 100 replicate runs).

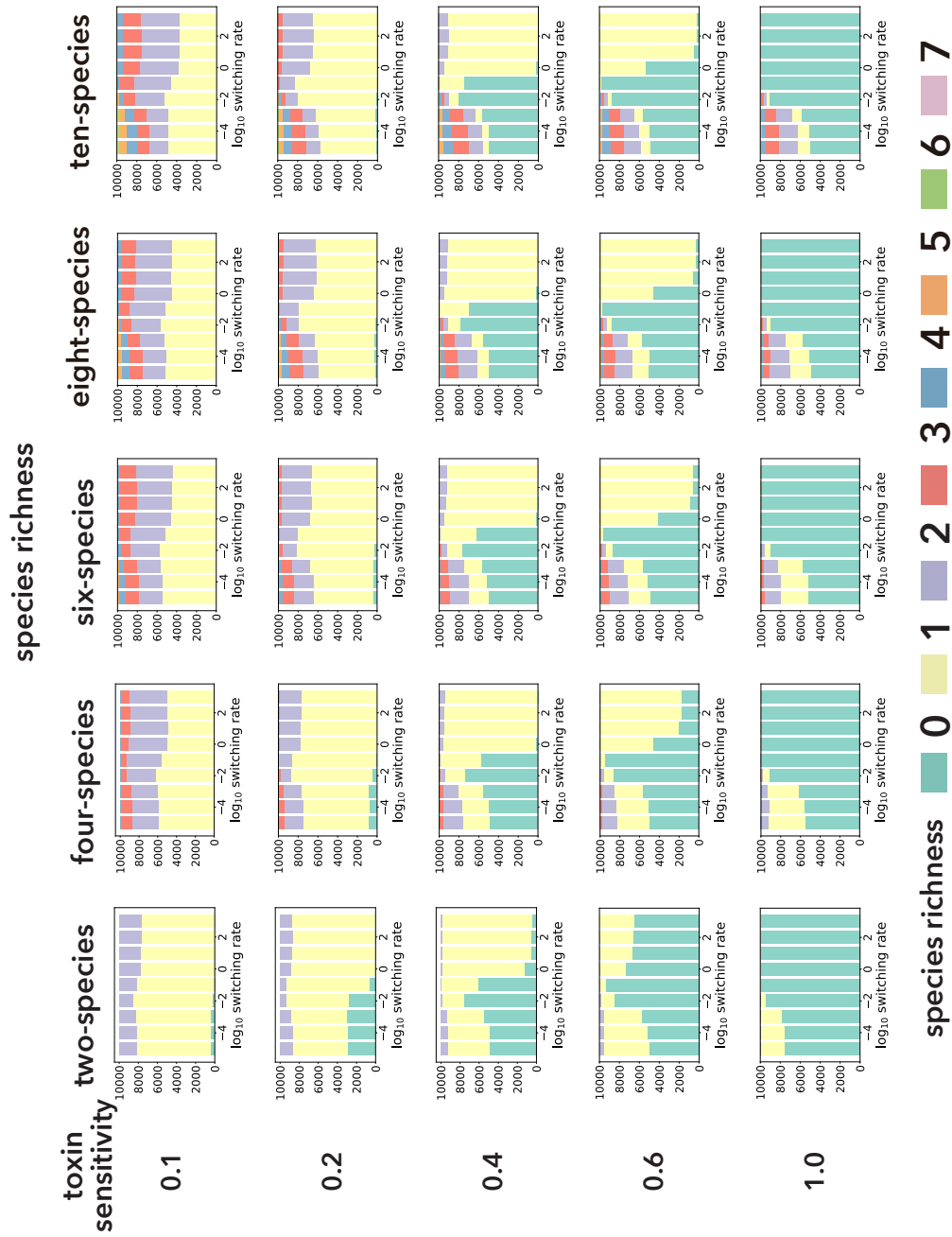


Figure A.11: Species richness with increasing initial number of species in a community

Species richness with increasing initial numbers of species  $N$  and mean toxin sensitivities  $\delta$ . Each bar plot represents results of  $10^4$  simulations.

Table A.1: List of fixed parameters in the interaction analysis

| Symbol        | Value  | Description   |
|---------------|--|---|
| $\alpha$      | 0.1  | dilution rate of the chemostat                                      |
| $R_1^\pm$     | $R_1^+ = 200, R_1^- = 50$                                    | abundant or scarce resource supply concentration                    |
| $T_1^\pm$     | $T_1^+ = 200, T_1^- = 50$                                    | abundant or scarce toxin supply concentration                       |
| $Y_{1k}^r$    | $Y_{1k}^r = 1$ for $k = 1, 2$                                | species $k$ 's biomass yields of resource                           |
| $Y_{1k}^t$    | $Y_{1k}^t = 1$ for $k = 1, 2$                                | species $k$ 's biomass yields of toxin                              |
| $\mu_{11}$    | 1.0  | maximum growth rate of species 1 on resource 1                      |
| $\mu_{12}$    | 0.91   | maximum growth rate of species 2 on resource 1                      |
| $\delta_{1k}$ | $[0.1, \dots, 1.0]$ and $\delta = \delta_{11} = \delta_{12}$ | sensitivity of species $k$ to toxin 1.                              |
| $K_{1k}^r$    | 100  | amount of resource 1 that gives half-max growth rate of species $k$ |
| $K_{1k}^t$    | 100  | amount of toxin 1 that gives half-max death rate of species $k$     |

Table A.2: Summary of critical toxin sensitivities and number of times non-monotonicity is observed

| Switching scenario                               |                | 1           | 2   | 3   | 1                |                    |                  |                    |
|--|----------------|-------------|-----|-----|------------------|--------------------|------------------|--------------------|
| Amounts of supplies                              |                | base line * |     |     | $\uparrow R_1^+$ | $\downarrow R_1^+$ | $\uparrow R_1^-$ | $\downarrow R_1^-$ |
| Critical toxin sensitivities                     | harsh          | 0.1         | 0.3 | 0.1 | 0.1              | 0.1                | 0.3              | 0.1                |
|  | mean           | 0.4         | 0.4 | 0.4 | 0.9              | 0.2                | 0.5              | 0.3                |
|  | mild           | 0.8         | 1.1 | 1.3 | 1.2              | 0.3                | 0.8              | 0.8                |
| number of non-monotonic changes observed between | mean and harsh | 2           | 0   | 2   | 7                | 0                  | 1                | 3                  |
|  | mean and mild  | 1           | 0   | 0   | 3                | 0                  | 0                | 2                  |
|  | mild and harsh | 3           | 0   | 2   | 10               | 0                  | 1                | 4 <sup>†</sup>     |

\* For exact parameter values, see Table A.1.

† At the critical toxin sensitivity corresponding to the mean environment ( $\delta = 0.3$ ), the species interaction non-monotonically changes over the switching rate: the frequency of non-monotonicity is  $3 + 2 - 1 = 4$ .